

# Detecting climate signals in populations across life histories

Stéphanie Jenouvrier<sup>1</sup>, Matthew C. Long<sup>2</sup>, Christophe F. D. Coste<sup>3</sup>,  
Marika Holland<sup>2</sup>, Marlène Gamelon<sup>3,4</sup>, Nigel G. Yoccoz<sup>5</sup> and Bernt-Erik Sæther<sup>3</sup>

## Affiliations:

1. Biology Department, Woods Hole Oceanographic Institution, Woods Hole, MA, USA
2. National Center for Atmospheric Research, Boulder, CO, USA
3. Centre for Biodiversity Dynamics, Department of Biology, Norwegian University of Science and Technology, 7491 Trondheim, Norway
4. Laboratoire de Biométrie et Biologie Évolutive, CNRS, Unité Mixte de Recherche (UMR) 5558, Université Lyon 1, Université de Lyon, Villeurbanne, France
5. Department of Arctic and Marine Biology, UiT The Arctic University of Norway, Tromsø, Norway.

**E-mail addresses:** Stéphanie Jenouvrier: [sjenouvrier@whoi.edu](mailto:sjenouvrier@whoi.edu);

Matthew C. Long: [mclong@ucar.edu](mailto:mclong@ucar.edu);

Christophe F. D. Coste: [christophe.f.d.coste@ntnu.no](mailto:christophe.f.d.coste@ntnu.no);

Marika Holland: [mholland@ucar.edu](mailto:mholland@ucar.edu);

Marlène Gamelon: [marlene.gamelon@univ-lyon1.fr](mailto:marlene.gamelon@univ-lyon1.fr),

Nigel Yoccoz: `nigel.yoccoz@uit.no`;

Bernt-Erik Sæther: `bernt-erik.sather@ntnu.no`.

**Statement of authorship:** SJ and ML developed the research ideas, conceptualized and designed the study. SJ performed modeling work and analyzed theoretical and empirical data. CC derived the mathematical equations. MH computed the sea ice forecasts. SJ wrote the first draft of the manuscript, and all authors contributed substantially to revisions.

**Data accessibility statement:** data are archived on the USAP-DC repository (dataset ID is 601491 and DOI is 10.15784/601491). Data are also archived on HAL, a public repository (hal-03468070).

**Running title:** Time of emergence in populations

**Keywords:** Time of emergence, signal to noise, climate change, life histories, population variability, population trend, emperor penguin.

**Type of article:** Reports

**Length:** The number of words in the abstract is 264. The number of words in the main text is  $\sim 9000$ . The number of references is 111. There are 8 figures, 3 tables.

**Corresponding author:** Stéphanie Jenouvrier

E-mail: `sjenouvrier@whoi.edu`

Telephone: (508) 289-3245

Fax: (508) 457-2169

Woods Hole Oceanographic Institution

266 Woods Hole Road,

Woods Hole, MA 02543-1050

U.S.A

## Abstract

Climate impacts are not always easily discerned in wild populations as detecting climate change signals in populations is challenged by stochastic noise associated with natural climate variability, variability in biotic and abiotic processes, and observation error in demographic rates. Detection of the impact of climate change on populations requires making a formal distinction between signals in the population associated with long-term climate trends from those generated by stochastic noise. The time of emergence (ToE) identifies when the signal of anthropogenic climate change can be quantitatively distinguished from natural climate variability. This concept has been applied extensively in the climate sciences, but has not been explored in the context of population dynamics. Here, we outline an approach to detecting climate-driven signals in populations based on an assessment of when climate change drives population dynamics beyond the envelope characteristic of stochastic variations in an unperturbed state. Specifically, we present a theoretical assessment of the time of emergence of climate-driven signals in population dynamics ( $ToE_{pop}$ ). We identify the dependence of  $ToE_{pop}$  on the magnitude of both trends and variability in climate and also explore the effect of intrinsic demographic controls on  $ToE_{pop}$ . We demonstrate that different life histories (fast species vs. slow species), demographic processes (survival, reproduction) and the relationships between climate and demographic rates, yield population dynamics that filter climate trends and variability differently. We illustrate empirically how to detect the point in time when anthropogenic signals in populations emerge from stochastic noise for a species threatened by climate change: the emperor penguin. Finally, we propose six testable hypotheses and a road map for future research.

# 1 Introduction

Climate change is expected to have significant effects on biological populations [Mason *et al.*, 2019]. Many studies have assessed the influence of particular climate variables on demographic rates (e.g., survival) and population sizes [e.g., see review Gaillard *et al.*, 2013; Jenouvrier, 2013; Reed *et al.*, 2021]. However, while the primacy of climate influence is commonly accepted, specific detection and attribution of population trends to anthropogenic changes in climate is complicated by substantial stochastic noise related to observation error (i.e., errors due to measurement imprecision) and process error in biological processes (i.e., unexplained variation in true abundance driven by unobserved biotic such as species interactions or abiotic processes such as habitat quality, resource variability...) and climate variability [Che-Castaldo *et al.*, 2017; Parmesan *et al.*, 2013] (Table 1). Climate variability is an important characteristic of the climate system and a driver of population dynamics [Boyce *et al.*, 2006; Vázquez *et al.*, 2015] that may occlude the population response to the underlying climate change signal.

Natural climate variability is noise from unforced variability generated internally within the climate system (Mann *et al.* [2021]) (Table 1). Natural variability in the climate system occurs over a broad range of temporal and spatial scales, with spectral properties in the seasonal, interannual to decadal bands. It arises from different sources, including variations that are (1) driven by a periodic external forcing, like the diurnal or the seasonal cycle of insolation, (2) due to the non-linear interplay of feedbacks within the climate system, such as coupled mode of variability (e.g. El Niño-Southern Oscillation, North Atlantic Oscillation, Pacific Decadal Oscillation), and (3) associated with random fluctuations in the external or internal climate system [Ghil, 2002]. In addition, climate change is characterized by an anthropogenic climate change signal (Table 1). This secular trend is the deterministic response of the climate system to an external forcing driven by anthropogenic emissions of greenhouse gases and changes in land use. Hence, the detection of

27 anthropogenic forced change is a signal to noise problem.

28 To detect and attribute the threats to a species posed by climate, climate-driven sig-  
29 nals in population should be distinguished from stochastic noise. The concept of time  
30 of emergence (ToE) exactly does that: it identifies when the signal of anthropogenic cli-  
31 mate change can be formally distinguished from noise associated with natural variability  
32 (Table 1). In climate science, the ToE has been studied extensively [Hawkins *et al.*, 2020;  
33 Hawkins & Sutton, 2012]. It is used to detect climatic changes and to describe whether  
34 climate changes are potentially beyond the known natural environmental variability of  
35 ecosystems [Giorgi & Bi, 2009; Mahlstein *et al.*, 2013].

36 Although, this concept of ToE has yet to be formally applied to ecological time se-  
37 ries, some studies have quantified when novel climate conditions relevant for ecological  
38 processes will emerge from natural variability. For example, Beaumont *et al.* [2011] have  
39 characterized the standard deviation (SD) of surface air temperature for a baseline pe-  
40 riod (1961-1990) and then evaluated the number of months that the temperature exceeds  
41 2 SDs by 2070 for various ecoregions of exceptional biodiversity. They found that more  
42 than 83% of terrestrial and freshwater ecoregions will be exposed to temperature exceed-  
43 ing 2 SDs by 2070.

44 The ToE explicitly characterizes the point in time when anthropogenic climate change  
45 can be formally distinguished from noise associated with natural variability. Hence, it  
46 informs on how fast changes exceed natural variability and can help prioritize decisions  
47 about when, where and for which conservation and management actions may be neces-  
48 sary. Some studies have characterized explicitly the ToE of ecosystem drivers in marine  
49 ecosystems [Henson *et al.*, 2017; Schlunegger *et al.*, 2020]. For example, Henson *et al.* [2017]  
50 found that climate change signals of pH and SST emerge rapidly while climate change  
51 trends in interior oxygen content and primary productivity emerge later. In terrestrial  
52 ecosystems, Rojas *et al.* [2019] focused on the timing when the precipitation changes will  
53 emerge outside the range of natural variability during the 21th century relevant for agri-

54 cultural activities. They found early timing of emergence in precipitation trends for the  
55 production regions of four major crops (wheat, soybean, rice, and maize) even under a  
56 low-emission scenario. Sorte *et al.* [2019] characterized the seasonal and spatial variations  
57 in the emergence of novel climates characterized by precipitation, minimum and maxi-  
58 mum temperature, along the migration routes of 77 passerine bird species. They found  
59 that earlier ToE occur for migrants that winter within the tropics. However, none of these  
60 studies have applied directly the concept of ToE to time series of population dynamics.

61 Here, we apply the concept of ToE to characterize climate-driven signals in popula-  
62 tion dynamics. We present a new perspective on detecting climate-related impacts in  
63 populations by characterizing the ToE in population growth rate (herefater,  $ToE_{pop}$ ), the  
64 point in time when climate-driven signals in population dynamics can be quantitatively  
65 distinguished from noise associated with year-specific stochastic variations in population  
66 growth rates (Fig. 1). While in climate science the noise is associated with climate nat-  
67 ural variability, applying this approach to population dynamics does not exclude other  
68 sources of noise (e.g., observation and process errors; demographic and environmental  
69 variability, the later being driven by fluctuations in physical habitat, resource availability,  
70 and biological interactions).

71 For species threatened by climate change,  $ToE_{pop}$  can represent the time at which the  
72 population will detectably decline to a level below its historical variability. This point  
73 in time potentially corresponds to the time at which the species will be exposed to high  
74 extinction risk, to the time at which individuals will migrate massively to track ecolog-  
75 ical niches, or to the time at which individuals may have to adapt to new conditions  
76 through evolutionary adaptations. The earlier the  $ToE_{pop}$  occurs, the faster novel condi-  
77 tions emerge out of the natural range of variability, the faster the population will reach  
78 a non-historical level, with less time for the organisms to adapt or migrate. The  $ToE_{pop}$   
79 is one illustrative metric that acknowledges the dual role of natural variability and an  
80 anthropogenic climate change signal, also useful for populations increasing under cli-

81 mate change [Román-Palacios & Wiens, 2020; Stephens *et al.*, 2016]. Importantly, ToE al-  
82 lows meaningful comparative studies of when the signal of anthropogenic climate change  
83 emerges from natural variability across ecosystem drivers [Henson *et al.*, 2017], species  
84 [Sorte *et al.*, 2019], ecosystems [Beaumont *et al.*, 2011] and for future socio-economic pro-  
85 cesses relevant for climate mitigation [Schlunegger *et al.*, 2020].

86 From a conceptual viewpoint,  $ToE_{pop}$  occurs earlier when the slope of the popula-  
87 tion climate-driven trend is large and/or when the population variability is small (Fig.  
88 1). Both the population climate-driven trend and variability depend on the species' life  
89 history and the functional relationships between climate and the demographic rates (Bar-  
90 raquand & Yoccoz [2013]). Specifically, species of both plant and animal kingdoms can  
91 be ranked along a main axis of life history variation, the so called "slow-fast continuum"  
92 [Gaillard *et al.*, 2016; Oli, 2004; Sæther, 1987; Salguero-Gómez *et al.*, 2016; Stearns, 1983].  
93 Species with fast life history are characterized by early maturity, high reproductive out-  
94 put and short lifespan; while species with slow life history have opposite characteristics.  
95 Previous work has shown that depending on their position along this continuum, species  
96 exhibit contrasting demographic responses to climate change with various spectrum of  
97 variability and amplitude of the response [Compagnoni *et al.*, 2021; Doak & Morris, 2010;  
98 Jenouvrier *et al.*, 2005; Morris *et al.*, 2008; Paniw *et al.*, 2017]. In addition, the population  
99 responses to climate change depend on the function that links climate variables to de-  
100 mographic rates (survival, growth, reproduction) that drive population growth rate and  
101 structure (i.e. functional relationships, Fig. S 1).

102 After briefly reviewing the time of emergence in climate (section 2), we present this  
103 concept in the context of population dynamics (section 3). Then, we characterize and  
104 compare the time of emergence of climate-driven signals in population dynamics in a  
105 theoretical context to address five questions (section 4):

- 106 • How does  $ToE_{pop}$  in populations relate to ToE in climate?
- 107 • How does  $ToE_{pop}$  vary across life histories (e.g. slow- fast species)?

- 108 • How does  $ToE_{pop}$  vary across demographic processes (e.g. survival, reproduction)?
- 109 • How does  $ToE_{pop}$  vary among different functional relationship between climate and
- 110 demographic rates?
- 111 • Do some species, demographic processes or functional relationship magnify the sig-
- 112 nal of anthropogenic climate change?

113 We find that different life histories (e.g., long vs. short-lived species) and demographic  
114 processes by which climate affects the population (i.e., through survival, reproduction)  
115 provide different “scale-dependent” filters so that some life histories magnify signal-to-  
116 noise ratios while other demographic dynamics prolong  $ToE_{pop}$ . Furthermore, to illustrate  
117 our theoretical results, we quantify the  $ToE_{pop}$  of an iconic species endangered by climate  
118 change: the emperor penguin (*Aptenodytes forsteri*) [Jenouvrier *et al.*, 2021] (section 5).  
119 Finally, we propose a set of six testable hypotheses based on the patterns of ToE in climate  
120 (hereafter  $ToE_{climate}$ ) and the demographic processes across life histories and propose a  
121 road map for future studies on the  $ToE_{pop}$  (section 6).

## 122 2 Time of emergence in climate

123 The concept of  $ToE_{climate}$  has been discussed for several decades in the climate sciences  
124 with studies attempting to detect the carbon dioxide warming signal published more than  
125 80 years ago ([Callendar, 1938; Revelle & Suess, 1957], see review in Hawkins *et al.* [2020]).  
126 The time of emergence has been characterized in temperature [Mahlstein *et al.*, 2011],  
127 precipitation [Giorgi & Bi, 2009], climate extremes [King *et al.*, 2015], in sea level [Lyu  
128 *et al.*, 2014], in Arctic climate [Landrum & Holland, 2020] and biogeochemical variables  
129 [e.g., Henson *et al.*, 2017; Long *et al.*, 2016; Schlunegger *et al.*, 2020].

130 Different methods have been used to quantify  $ToE_{climate}$ , most of them using climate  
131 model simulations (but see Hawkins *et al.* [2020] for an application using observation  
132 of temperature). The common methods for estimating  $ToE_{climate}$  are the signal threshold

133 method (section 3), and the signal-to-noise ratio method with a particular cutoff [Hawkins  
134 & Sutton, 2012]; a variant of this approach is the identification of the signal-to-noise ra-  
135 tio using a predefined threshold across multiple consecutive years (referred as the ex-  
136 ceedance threshold) [Mora *et al.*, 2013]. Various statistical methods have been developed,  
137 from statistical test to assess for significant differences between time periods [Zappa *et al.*,  
138 2015], estimation of the standard error of the regression to estimate the lead-time required  
139 for a linear trend to emerge from natural variability [Mahlstein *et al.*, 2012], development  
140 of hierarchical statistical state-space model [Barnhart *et al.*, 2016] or artificial neural net-  
141 works [Barnes *et al.*, 2018].

142 Recently, the availability of large ensembles of climate (or Earth system) models have  
143 open new doors to quantify climate natural variability and hence evaluations of the  $ToE_{climate}$ .  
144 An ensemble is a collection of coupled climate simulations (Table 1) that are integrated  
145 in parallel, typically with small differences in initial conditions applied to each ensemble  
146 member. Climate model generate internal variability as a product of interactions between  
147 components internal to the climate system [Hasselmann, 1976]. Since the climate system  
148 is chaotic, perturbations in initial conditions grow with time, randomizing the phase of  
149 natural variability and leading to spread across the ensemble. This spread can be inter-  
150 preted as a measure of the amplitude of natural climate variability. As all the ensemble  
151 members are subject to the same external forcing (i.e., emissions scenario), the determin-  
152 istic response of the climate system can be assessed as the mean across the ensemble  
153 members, which effectively filters out the noise associated with natural variability [Kay  
154 *et al.*, 2015]. Modeling centers usually contribute a small number of ensemble members  
155 to international climate change projection assessments, typically ranging from 3 to 10 en-  
156 semble members for a given model. Large ensembles with ensemble sizes ranging from  
157 30 to 100 members permit climatologists to compute emergence thresholds to formally  
158 consider the uncertainty in the forced response due to natural climate variability [Barn-  
159 hart *et al.*, 2016].

160 Here, we use signal threshold method (section 3) based on a large ensemble by con-  
161 structing prediction interval of the climate and population projections, and estimate the  
162 time taken by the system to emerge from the background of natural variability [Barnhart  
163 *et al.*, 2016]. For example, the left part of Figure 2 shows an idealized climate trajectory  
164 corresponding to a single ensemble member (red line) and the associated envelope of nat-  
165 ural variability based on a 95% prediction interval (gray).  $ToE_{climate}$  is the time when the  
166 projected future conditions under the influence of climate change, “forced conditions”  
167 (red lines), exceeds a pre-defined threshold for emergence that is based on the histori-  
168 cal unperturbed conditions (gray area, with the horizontal line illustrating the baseline  
169 threshold at which climate change is defined to emerge).

170 The emergence thresholds are typically based on the percentile of the distribution of  
171 the historical and forced projections. They define the prediction intervals at which the  
172 signal of climate change emerges from the natural climate variability. We present the re-  
173 sults for one threshold of wide confidence envelope with a 95% prediction interval based  
174 on emergence thresholds defined by the 2.5 or 97.5 percentile values of the distribution,  
175 where impacts are triggered by the extreme historical conditions only. The analysis with a  
176 narrow confidence envelope with emergence thresholds defined by the 20 or 80 percentile  
177 values of the confidence interval (i.e. 60% prediction interval) is shown in appendix (Fig.  
178 S 3). In that case, the system is likely highly sensitive to climate as severe impacts are  
179 thought to occur for lower percentile of the climate conditions distribution experienced  
180 during the historical run. Our results are qualitatively the same between 95% and 60%  
181 prediction intervals (Figs. 3 versus S 3).

182 In our simulations, we construct a large ensemble of climate time series for both the  
183 historical and forced environment for various natural climate variability ( $\sigma^2$ ) and warm-  
184 ing trends ( $\alpha$ ). Specifically, the historical climate time series are obtained by sampling  
185 into a normal distribution – centered on a zero mean and with a specific standard devia-  
186 tion  $\sigma$  – with independent draws each year (i.e. Independent and Identically Distributed

187 random variables (IID)). The forced climate time series are calculated by adding to this  
188 natural variability a linear trend of slope  $\alpha$ . In that context, this ToE calculation in an  
189 IID environment is directly related to the signal-to-noise ratio:  $ToE = \frac{2P}{SNratio}$  with P the  
190 climate value corresponding the threshold of the prediction interval.

191 In our theoretical study, we explore a range of parameters consistent with the observed  
192 standard deviation of the inter-annual temperature variability (Fig. 1 of Hawkins & Sut-  
193 ton [2012]) and the projected climate warming by 2100 (IPCC), with  $\sigma_C \in [0.2 \ 1.5]$  and  
194  $\alpha_C \in [0.01 \ 0.15]$  (Fig. 2). In our empirical example, we used 40-members from the Com-  
195 munity Earth System Model Large Ensemble (CESM-LE, Kay *et al.* [2015]) to characterize  
196 the confidence envelope of sea ice, hence the  $ToE_{climate}$  and  $ToE_{pop}$ .

### 197 **3 Conceptual model of the time of emergence in popula-** 198 **tion**

199 The time of emergence depends both on (1) the time varying signal,  $T(t)$  estimated as  
200 the long term monotonic trend (red trend on Fig. 1) and (2) the noise based on the range of  
201 natural variability over some historical period (variations of the black time series on Fig.  
202 1, section 2). Hence, it is important to understand how the climate-driven trend in pop-  
203 ulation growth rate and its year-specific stochastic variations are related to climate trend  
204 and variability (section 3.2, Fig. 1). Although, previous theoretical studies have shown  
205 that the variance in annual population growth rates depends on the variance in climate  
206 in a stationary environment [Engen *et al.*, 2005], we still lack a theoretical understanding  
207 on how the population trend and variability respond to climate in a non-stationary en-  
208 vironment. Hence, after introducing the methods to estimate the time of emergence in  
209 population (section 3.1), we discuss conceptually the links between the trend and vari-  
210 ability of population and climate (section 3.2, Fig. 1). In addition, to partially shedding  
211 light on those concepts, we build on previous theoretical studies [Engen *et al.*, 2005; Morris  
212 *et al.*, 2008] to show analytically how the variance in annual population growth rates can

213 be related (linearly for small environmental changes) to the climate variance in a stochas-  
214 tic and stationary environment by explicitly accounting for the functional relationship  
215 between climate and demographic rates (section 3.3, eq. 8).

### 216 **3.1 Methods to estimate $ToE_{pop}$**

217 As in climate (section 2), population ecologists can use various methods to estimate the  
218 time of emergence in population  $ToE_{pop}$ . Figure 2 illustrates the signal threshold method  
219 used here (section 2), where the time of emergence is the first year when the projected fu-  
220 ture state of a variable crosses a pre-defined emergence threshold based on the historical  
221 variations. For example, the projected future state of a population can be depicted by the  
222 gray envelope of future projections (red lines on Figs. 1, 2) under a specific forcing sce-  
223 narios based on a range of emissions of greenhouse gases (GHGs), while the emergence  
224 threshold can be determined from the gray envelope of historical population projections  
225 (black lines on Figs. 1, 2)).

226 In ecological impact studies, the emergence threshold (e.g., horizontal lines on Figs. 1,  
227 2) can be interpreted as thresholds beyond which management-relevant impacts will oc-  
228 cur and depend on the management sensitivity to changes in climate conditions. Indeed,  
229 emergence thresholds are not necessarily set at the extreme 2.5% high or 2.5% low of the  
230 range of historical population variations ( $\sim 2\sigma$ ) usually used in risk impact studies but  
231 can be set at any thresholds at which the decline or increase in population is perceived as  
232 unsustainable. For example, high management sensitivity threshold may be desirable for  
233 increasing species, whereby management actions are triggered by low emergence thresh-  
234 olds e.g. 60% prediction interval of population growth distribution during the baseline  
235 period (Fig. S 3).

### 236 **3.2 Factors influencing the $ToE_{pop}$**

237 Figure 2 shows that the time of emergence in populations varies among species. From  
238 a conceptual viewpoint, this depends on the sensitivity of the population growth rate  
239 to climate:  $\frac{\partial\lambda}{\partial C}$  (Fig. 1). This sensitivity can be decomposed into two main components.

240 First, it depends on the sensitivity of the demographic rates themselves  $\theta_i$  (e.g. survival,  
 241 reproduction) to climate  $\frac{\partial \theta_i}{\partial C}$  (panel 1 in the demographic rates box on Fig. 1). Therefore,  
 242 the functional relationships between climate and the demographic rates likely play a key  
 243 role in the sensitivity of the population growth rate to climate. Second,  $\frac{\partial \lambda}{\partial C}$  depends on  
 244 the sensitivity of the population growth rate to demographic rates  $\frac{\partial \lambda}{\partial \theta_i}$  (panel 2 in the  
 245 demographic rates box on Fig. 1). The latter is influenced by the species' life history  
 246 [Saether & Bakke, 2000]. For instance, the "demographic buffering" hypothesis posits  
 247 that in long-lived species, adult survival is expected to be buffered against environmental  
 248 changes (environmental canalization sensu Gaillard & Yoccoz [2003]) and reproduction  
 249 is expected to be more variable with stronger functional relationships with climate. The  
 250 opposite patterns are expected in short-lived species (see Hilde *et al.* [2020] for a review).  
 251 Therefore, demographic rates of species with contrasting life histories are expected to  
 252 be differently influenced by climate, influencing in turn the sensitivity of the population  
 253 growth rate to climate, the variance in annual population growth rates and the climate-  
 254 driven change in population. As a result, time of emergence in populations is expected to  
 255 vary among species, but the pattern of such variations are difficult to predict conceptually.  
 256 Indeed, in next section, we show that the magnitude of the demographic response to  
 257 climate (i.e.  $\frac{\partial \theta_i}{\partial C}$ ) increase both the variance and the climate-driven trend of the population,  
 258 with effect size that vary with the mean state of climate (see Supplementary Appendix 1  
 259 and Fig. 1), hence unknown resulting impact on  $ToE_{pop}$ .

### 260 3.3 Population variability in a stationary environment

261 In this section,, we show how the variance in annual population growth rates depends  
 262 on the variance in climate,  $\sigma^2$ , and the functional relationship between the mean climate  $\bar{C}$   
 263 and demographic rates, assuming a stationary environment (i.e., one in which the mean  
 264  $\bar{C}$  and variance  $\sigma^2$  do not vary over time). For a structured population model of the  
 265 form  $\mathbf{n}_{t+1} = \mathbf{A}_t \mathbf{n}_t$  (see section 4, Fig. 1) in a stationary environment characterized by  
 266 small variations, the environmental variance of the population growth rate  $\lambda_t$  (such that

267  $N_{t+1} = \lambda_t N_t$ ) can be approximated (first degree Taylor approximation) by [see Engen *et al.*,  
 268 1998, 2005]:

$$\text{var}(\lambda_t) = \sum_{i,j} \frac{\partial \lambda}{\partial \theta_i |_{\theta_i = \bar{\theta}_i}} \frac{\partial \lambda}{\partial \theta_j |_{\theta_j = \bar{\theta}_j}} \text{Cov}(\theta_i, \theta_j) \quad (1)$$

269 with  $\bar{\theta}$ , the vector of mean demographic parameters including fertility, survival of juve-  
 270 niles and adult and maturation rates (Table 1).

271 This variance is important as it influences the long-term stochastic growth rate of the  
 272 population:

$$\log \lambda_s = \lim_{T \rightarrow \infty} \frac{1}{T} \log \|\mathbf{A}_{T-1} \cdots \mathbf{A}_0 \mathbf{n}(0)\|. \quad (2)$$

273 Let us assume that the environment affects only one demographic rate,  $\theta_i$  (the other rates  
 274  $\theta_j$  remain constant over time), then Eq 1 simplifies as:

$$\text{var}(\lambda_t) = \left( \frac{\partial \lambda}{\partial \theta_i |_{\theta_i = \bar{\theta}_i}} \right)^2 \text{var}(\theta_{it}). \quad (3)$$

275 The demographic rate  $\theta_i$  is a function of a climatic variable  $C_t$ .  $\theta_i$  is also affected by  
 276 other unknown variables generating environmental stochasticity  $\epsilon$ , such as observation  
 277 and process errors.  $\epsilon$  is a stochastic environmental noise of mean 0, and variance  $\text{var}(\epsilon_t)$   
 278 and is considered as an additional variability independent from  $C$ . For example, let's  
 279 assume that  $\theta_i$  is an inverse logit function of a linear function of  $C$ :

$$\theta_{it} = \theta_i(C_t, \epsilon_t) = g(y = \beta_0 C_t + \beta_1 + \epsilon_t), \quad (4)$$

280 where  $\beta_0$  and  $\beta_1$  are the constant regression coefficient of the functional relationship be-  
 281 tween climate and the demographic rate (Fig. 1);  $g$  is the inverse logit link function so that  
 282  $\theta_i \in [0, 1]$ . Applying the second order Taylor expansion, the variance of the demographic  
 283 rate  $\theta_i$  is:

$$\text{var}(\theta_{it}) \approx (g'(\bar{y}))^2 \text{var}(y) = \left( \frac{\partial \theta_i}{\partial C} \Big|_{C=\bar{C}} \right)^2 (\beta_0^2 \sigma^2 + \text{var}(\epsilon_t)^2) \quad (5)$$

284 with  $\sigma^2$  the variance of the climatic variable  $C$  and

$$\frac{\partial \theta_i}{\partial C_{C=\bar{C}}} = y' \frac{\exp(-y)}{(1 + \exp(-y))^2} = \beta_0 \frac{\exp(-\beta_0 \bar{C} - \beta)}{(1 + \exp(-\beta_0 \bar{C} - \beta_1))^2} \quad (6)$$

285 .

286 Hence Eq 3 can be simplified as:

$$\text{var}(\lambda_t) = \left( \frac{\partial \lambda}{\partial \theta_{i|\theta_i=\bar{\theta}_i}} \right)^2 \left( \frac{\partial \theta_i}{\partial C}_{|C=\bar{C}} \right)^2 (\beta_0^2 \sigma^2 + \text{var}(\epsilon_t)^2). \quad (7)$$

287 Applying the derivative chain rule and assuming  $\epsilon = 0$ , i.e., that the demographic rate  
288  $\theta_i$  is a deterministic function of climate, like in our simulations, we obtain:

$$\text{var}(\lambda_t) = \beta_0^2 \sigma^2 \left( \frac{\partial \lambda}{\partial C}_{|C=\bar{C}} \right)^2 \quad (8)$$

289 Hence the year-specific stochastic variation depends on climate internal variability  
290  $\sigma^2$ , the stochastic environmental variability, as well as the sensitivity of the population  
291 growth rate to the demographic rate and the sensitivity of the demographic rate to climate  
292 in a stationary environment that both define the overall the sensitivity of the population  
293 growth rate to climate.

294 In a non-stationary environment (Fig. 1),  $\bar{C}$  is changing, and  $\text{var}(\lambda)$  varies, in general,  
295 non-linearly with  $\bar{C}$  depending on the sensitivity of the population growth rate to climate  
296  $\left( \frac{\partial \lambda}{\partial C} \right)$  (see Supplementary Appendix 2 and Fig. 1), this latter also influences the population  
297 trend. Hence, it is difficult to posit *a priori* how  $\text{ToE}_{\text{pop}}$  will vary with the signal and  
298 noise in climate across life histories and demographic processes for various functional  
299 relationship between climate and demographic rates. In section 4 we use a simulation  
300 framework to answer our five questions posed in the introduction, and discuss six testable  
301 hypotheses in section 6.

## 302 4 Time of emergence in populations

### 303 4.1 Population projections

304 To project the population dynamics of species with four contrasting life histories along  
305 the slow-fast gradient (Table 2), we use a simple two-stage climate-dependent population  
306 matrix model that permits to explore some of the diversity of life cycles (Caswell [2001];  
307 Neubert & Caswell [2000], Fig. 1). The model distinguishes non-reproducing juveniles  
308 and reproducing adults (see life cycle on Fig. 1). The population is projected from year  $t$   
309 to year  $t+1$  by:

$$\mathbf{n}_{t+1} = \mathbf{A}(\theta[(\mathbf{C}_t)])\mathbf{n}_t \quad (9)$$

310 with  $\mathbf{n}_t$  the population vector made of the abundances of juveniles and adults and  $\mathbf{A}$   
311 the population transition matrix including demographic rates  $\theta[(\mathbf{C}_t)]$  that are defined by  
312 specific functional relationship with climate  $C$  (Figs. 1, S 1). The demographic rates are  
313 the survival of juveniles  $S_j$  and adults  $S_a$ , the development rate of juveniles into adults  $\gamma$   
314 (maturation rate), and the fertility of adults  $F$ .

$$\mathbf{A} = \begin{bmatrix} S_j(1 - \gamma) & F \\ S_j\gamma & S_a \end{bmatrix} \quad (10)$$

315 This model permits the simulation of population dynamics of species with four con-  
316 trasting life histories with increasing generation time (the mean age of mothers at child  
317 birth), which is a reliable metric to rank species along the continuum of life history varia-  
318 tion [Gaillard *et al.*, 2005]). Species differ in terms of reproductive strategy (semelparous  
319 vs. iteroparous), age at first reproduction (precocial vs. delayed) [Neubert & Caswell,  
320 2000] and lifespan (short vs. long) and thus range along the slow-fast continuum of life  
321 history variation [Gaillard *et al.*, 2016] from fast species with short generation time, high  
322 reproductive output and short lifespan (species 1) to slow species with opposite char-  
323 acteristics (species 4) (Table 2). For example, species 1 represents organisms with rapid

324 life cycle development, only one reproductive event in their lifetime and high fecundity  
 325 ( $b \sim 168$ ) (Table 2), such as many annual plants and insects. Species 2 are short-lived  
 326 iteroparous species producing 7-8 offspring per unit time per female such as small mam-  
 327 mals and birds. At the other end of the spectrum, species 4 are long-lived species with  
 328 delayed first reproduction, low reproductive output per breeding event and long lifes-  
 329 pan such as primates, whales, or albatross. While these species do not capture the full  
 330 diversity of life history, especially for plants that exhibit a vast amount of life-history  
 331 variations, they provide a reasonable sample of characteristic traits across a representa-  
 332 tive range. Indeed, Salguero-Gómez *et al.* [2016] showed that the first axis of life-history  
 333 variations of 418 plant species worldwide representing the slow-fast continuum explains  
 334 34% of the variation in plant life-history strategies, while it explains even a higher per-  
 335 centage of variations (60–80%) among mammals [Oli, 2004], birds [Sæther, 1987], and  
 336 reptiles [Bauwens & Diaz-Uriarte, 1997].

337 We include the effects of climate acting on only one demographic parameter at a time  
 338  $\theta_i$  and assume that the inter-annual variability in population growth rates is induced by  
 339 climate only (i.e.  $\epsilon = 0$  in eq.7). In each case, the functional relationship between demo-  
 340 graphic rates and climate  $\theta_i(C)$  is either linear, sigmoid or a bell shaped curve functions  
 341 (Fig. 1, Fig. S 1) and is defined by the equation 4 with  $\epsilon = 0$  and  $\beta_1 = \overline{\theta_{ih}}$  the mean  
 342 demographic parameter in the historical unperturbed environment that leads to a stable  
 343 population with  $\overline{C} = 0$  (Table 1). Specifically, relationships can be linear functions on the  
 344 real scale, with

$$\theta_i(C_t) = \beta_0 C_t + \overline{\theta_{ih}} \quad (11)$$

345 and results are shown only on supplementary figure S 4 for all demographic rates. Rela-  
 346 tionships can be sigmoid functions, with

$$\theta_i(C_t) = g(y = \beta_0 C_t + \overline{\theta_{ih}}) \quad (12)$$

347 and  $g$  the inverse logit link function. Relationships can be bell shaped curves functions  
 348 with quadratic functional relationship between demographic rate and climate:

$$\theta_i(C_t) == g(y = \beta_0 C_t^2 + \overline{\theta_{ih}}) \quad (13)$$

349 For most demographic rates,  $g$  is the inverse logit link function so that  $\theta_i \in [0, 1]$ , but not  
 350 for fertilities of species 1 to 3 that vary on the real scale.

351 To characterize a reasonable range of demographic rates and lifetime outcomes in the  
 352 set of projected environmental conditions,  $\beta_0$  vary in a specific range that depends on  
 353 the functional relationship. For linear functional relationships between climate and de-  
 354 mographic parameters (equation 11), the slope varies as:  $\beta_0 \in [-0.03, 0.03]$  (Fig. S 4).  
 355 For sigmoid functional relationships the slope varies as:  $\beta_0 \in [-0.15, 0.15]$  (Fig. 3a). For  
 356 bell-shaped functional relationships the slope vary as:  $\beta_0 \in [-0.025, -0.01]$  (Fig. 3b).

357 We calculate the time of emergence of population using the threshold methods fol-  
 358 lowing the same methodology as for climate (section 2). We assume that the historical  
 359 population is stable in an unperturbed stationary environment with  $\overline{C} = 0$  and variance  
 360  $\sigma^2$ ; i.e. the stochastic long-run growth rate is null:  $\ln(\lambda_s) = 0$  (calculated from equation 2).  
 361  $\ln(\lambda_s)$  depends on variance in annual population growth rates  $\text{var}(\lambda)$  [Lande *et al.*, 2003;  
 362 Tuljapurkar & Orzack, 1980] that is driven by the natural climate variability  $\sigma^2$  (section  
 363 3). Climate fluctuations that increase the variance of demographic rates usually decrease  
 364 the stochastic long-run growth rate of populations [Engen *et al.*, 2005; Lande *et al.*, 2003;  
 365 Tuljapurkar, 1982]. Hence, to set  $\ln(\lambda_s) = 0$  across environmental historical conditions, the  
 366 vector of demographic parameters  $\theta$  is slightly tuned for each environmental variability  
 367  $\sigma$ .

## 368 4.2 Time of emergence in population depends on climate variability and trend

369 We found that  $\text{ToE}_{\text{pop}}$  can be predicted by the climate signal-to-noise ratio and occurs  
 370 earlier as the signal-to-noise in climate becomes larger (Fig. 3). Indeed, the  $\text{ToE}_{\text{pop}}$  is

371 linearly and positively correlated to the  $ToE_{climate}$  (Fig. 3) as both the variability and trend  
372 in population are positively related to the natural variability and trend of climate (Fig. 4).

373 Remarkably, the  $ToE_{pop}$  can be earlier or later than the  $ToE_{climate}$ , depending on the life  
374 history strategies and the demographic processes by which climate affects demographic  
375 rates (Fig. 3). For example, the  $ToE_{pop}$  is earlier than  $ToE_{climate}$  for iteroparous species for  
376 which climate affects maturation or adult survival rates for long-lived species (species  
377 3 & 4) or juvenile survival for short-lived species (species 2). Hence, some life histories  
378 may permit an earlier detection of the time at which the signal of anthropogenic climate  
379 change emerges from the noise of natural climate variability

### 380 **4.3 Time of emergence in population across life histories and demographic processes**

381 The  $ToE_{pop}$  can be predicted by life histories and demographic processes (Fig. 3, Fig. 5).  
382 Across life histories, the  $ToE_{pop}$  is the largest for species 1 (semelparous short-lived strat-  
383 egy), which have on average the largest population variations (Table 2, Fig. 5). Across  
384 demographic processes, the  $ToE_{pop}$  is the longest for the fertility (Table 2). For iteroparous  
385 species, the  $ToE_{pop}$  depends on the sensitivity of the population growth rate to the demo-  
386 graphic rate affected by climate and occurs earlier as the sensitivity increases (Fig. 5). As  
387 a consequence, the  $ToE_{pop}$  occurs later as species longevity increases when climate affects  
388 fertility and juvenile survival. However, the opposite pattern occurs when climate affects  
389 adult survival and maturation rate:  $ToE_{pop}$  occurs earlier for long-lived than short lived  
390 species (Fig. 3, Table 2).

### 391 **4.4 Time of emergence in population among different functional relationships be-** 392 **tween climate and demographic rates**

393 Surprisingly, the type of functional relationship between climate and demographic rates  
394 and its slope have little effect on the  $ToE_{pop}$  (Fig. 3, Fig. 6). While the variability of the pop-  
395 ulation in the historical environment is smaller for bell shape versus linear relationships  
396 (see eq 9 section 3), both the trend and variability are larger for bell shape relationship  
397 in the non-stationary forced environment (Table 3). Indeed, the variability in the forced

398 environment increases substantially compared to the variability in the historical environ-  
399 ment for bell shape, while it does not change for linear relationships (Table 3). However,  
400 the ratio of the trend to the magnitude of variability is very similar between bell shape  
401 and linear relationship, and the patterns of time of emergence are thus very similar re-  
402 gardless of the shape of the functional relationship. The slope of those relationships has  
403 also little impact of the  $ToE_{pop}$  relative to life histories and demographic processes, prob-  
404 ably because it affects both the trend and variability simultaneously (Fig. 1).

## 405 **5 Time of emergence of emperor penguin population**

406 The emperor penguin is a relevant example to test our theoretical predictions, specif-  
407 ically that long lived species (comparable to species 4) may permit an earlier detection  
408 of anthropogenic climate change influences in population growth rates (Fig. 3, section  
409 4.2). Penguins are threatened by future climate change as they rely on sea ice for breeding  
410 substrate and warming is driving reductions in sea ice cover [Jenouvrier *et al.*, 2020, 2014,  
411 2021]. Adult survival is strongly affected by sea ice during four seasons of the life cycle  
412 resulting in complex, non-linear bell shape relationships [Jenouvrier *et al.*, 2012]. Adult  
413 survival is maximized at intermediate levels of sea ice because neither the complete ab-  
414 sence of sea ice (low food resources and/or high predation), nor heavy and persistent sea  
415 ice (longer foraging trips), provide satisfactory conditions. Thus, in contrast to our the-  
416 oretical examples, relationships between climate and demographic rates are even more  
417 complex for the emperor penguin. Indeed, sea ice affects a multitude of demographic  
418 rates during various seasons, with different functional responses among sexes. Further-  
419 more, other processes contribute to the variability in population growth rate (i.e.  $\epsilon \gg 0$   
420 in eq.7, related to sampling variance and process variance due to unmeasured environ-  
421 mental conditions such as local fast ice dynamics or large-scale atmospheric perturbations,  
422 see Trathan *et al.* [2020] for a review).

## 423 5.1 Emperor penguin life cycle

424 The life cycle of emperor penguins includes 5 stages according to breeding status and  
425 sex (Fig. 7): male and female pre-breeders (birds that have yet to breed for the first time),  
426 breeding pairs, and male and female non-breeders (birds that have bred before but do  
427 not do so in the current year). The demographic rates describing the transitions between  
428 these stages from year  $t$  to  $t + 1$  includes: the probability that an individual of a given  
429 stage returns to the breeding site, the probability of mating as a function of the availability  
430 of potential mates, the probability of breeding success (raising an offspring given that the  
431 female lays an egg), the primary sex ratio (fixed at 0.5), the survival of offspring during  
432 the first year at sea, and the annual survival of pre-breeders, non-breeders and male and  
433 female breeders.

434 The functional relationships between demographic parameters and sea ice concentra-  
435 tion anomalies depend on four seasons (described in detail in Jenouvrier *et al.* [2012]):

- 436 1. The non-breeding season from January to March,
- 437 2. The arrival, copulation and laying period (April–May), hereafter called the laying  
438 period,
- 439 3. The incubation period (June–July),
- 440 4. The rearing period (August–December).

441 Relationships are sigmoid functions, with linear ( $\beta_2 = 0$ ) or quadratic functional relation-  
442 ship between demographic rate and sea ice  $\mathbf{x}$  on the logit scale:

$$\theta_i(\mathbf{x}(t)) == g(y = \beta_0 + \beta_1\mathbf{x}(t) + \beta_2\mathbf{x}(t)^2 + \epsilon_t) \quad (14)$$

443 including the parameter estimates  $\beta_k$  and the environmental stochasticity  $\epsilon$  generated by  
444 other unknown variables.  $\epsilon$  is a stochastic environmental noise of mean 0, and variance

445  $\text{var}(\epsilon_t)$  and is considered as an additional variability independent from sea ice.  $g$  is the  
446 inverse logit link function so that  $\theta_i \in [0, 1]$ .

## 447 **5.2 Emissions scenario, climate model and climate outputs**

448 The climate outputs from multiple AOGCMs (Atmosphere Ocean General Circulation  
449 Model) are publicly available in a standardized format on the Coupled Model Intercom-  
450 parison Project (CMIP) website. CMIP5 provides a framework for coordinated climate  
451 change experiments for assessment in the IPCC Fifth Assessment Report (AR5) in 2014  
452 using four Representative Concentration Pathways (RCP) describing future GHG con-  
453 centration trajectories based on socio-economic assumptions. Newer emissions forcing  
454 scenarios have been developed and used for climate projections in CMIP6 for the Sixth  
455 Assessment Report (AR6) released in August 2021. These “Shared Socioeconomic Path-  
456 ways” [O’Neill *et al.*, 2016](SSPs) differ in the time evolution of specific climate forc-  
457 ers such as GHG and aerosol emissions, but bracket the same range in energy flux varia-  
458 tions in the atmosphere caused by anthropogenic factors of climate change (i.e., radiative  
459 forcing range) as the RCP scenarios.

460 There are several sources of uncertainties in climate projections that affect the time  
461 of emergence, including the structural uncertainty associated with the different climate  
462 models used to make projections, and the scenario uncertainty associated with different  
463 future emission pathways [Deser *et al.*, 2012; Hawkins & Sutton, 2009; Schlunegger *et al.*,  
464 2020]. However, here we use one climate model and one scenario to obtain the sea ice  
465 outputs from a large ensemble [Kay *et al.*, 2015] for illustrative purposes, as large ensem-  
466 ble simulations using several scenarios from several climate models were not available at  
467 the time of our analysis.

468 Specifically, we used RCP 8.5 high emission scenario [Meinshausen *et al.*, 2011], that  
469 represents a future in which greenhouse gas emissions continue unabated. RCP 8.5 is con-  
470 sidered as a useful scenario for quantifying physical climate risk, especially over near- to  
471 midterm policy-relevant time horizons [Schwalm *et al.*, 2020]. Indeed, the total cumula-

472 tive CO<sub>2</sub> emissions since 2005 projected under RCP8.5 by 2020 are in close agreement with  
473 historical observed total cumulative CO<sub>2</sub> emissions [Schwalm *et al.*, 2020]. In addition,  
474 the total cumulative CO<sub>2</sub> emissions since 2005 projected under RCP8.5 by 2050 agree well  
475 with energy forecasts under current and stated policies by 2050, with still highly plausible  
476 levels of CO<sub>2</sub> emissions by 2100 [Schwalm *et al.*, 2020].

477 We use sea ice outputs from a large ensemble produced by the Community Earth  
478 System Model (CESM), development of which is coordinated by the National Center for  
479 Atmospheric Research (NCAR), allowing us to characterize the natural climate variability  
480 [Kay *et al.*, 2015]. In addition, the CESM model resolves very well the Antarctic sea ice  
481 conditions that influence the most emperor penguin population growth rates [Jenouvrier  
482 *et al.*, 2020].

### 483 5.3 Sea ice and penguin projections

484 We calculate  $ToE_{pop}$  for the 54 known colonies around the coast of Antarctica ([Fretwell  
485 *et al.*, 2012; Fretwell & Trathan, 2009], Fig. S 7) following the approach outlined in section  
486 2 based on projections of population growth rates driven by sea ice changes. Specifically,  
487 to project emperor penguin population growth rate at each colony, we link a climate-  
488 dependent demographic matrix model to sea ice projections (section 5.2). Our sea ice-  
489 dependent demographic model includes demographic rates that depend on the sea ice  
490 conditions during four seasons (non-breeding, laying, incubating and rearing, section 5.1  
491 ), and accounts for differences in the impact of sea ice conditions on adult survival be-  
492 tween sexes (see Supporting information S3 for more details). These relationships and  
493 their estimations are described in detail in Jenouvrier *et al.* [2012]. The model includes  
494 sources of stochasticity and uncertainties: (1) parameter uncertainty describes statisti-  
495 cal uncertainty in the estimates of demographic parameters (e.g., survival, and their re-  
496 sponses to sea ice concentration anomalies) and (2) process variance (i.e., environmental  
497 stochasticity) reflects true “unexplained” temporal variance in demographic rates that is  
498 not accounted for by sea ice, which combined reflect the term  $var(\epsilon)$  in eq.7, section 3. As

499 we ignored these context specific uncertainties in our theoretical simulation, we present  
500 the results with two scenario: with or without  $\text{var}(\epsilon)$ .

501 For our historical environment we used sea ice projections from 1920-1950, and for  
502 the forced environment we used sea ice projections from 1950-2100 under climate sce-  
503 nario RCP 8.5 (section 5.2). We assume that the population is stable in the historical,  
504 unperturbed environment and our emergence threshold are based on the 95% prediction  
505 interval. This permit us to characterize when anthropogenic signals in emperor penguin  
506 populations are *very likely* to emerge from stochastic noise.

#### 507 **5.4 Time of emergence in sea ice and penguin**

508 The  $\text{ToE}_{\text{climate}}$  in sea ice varies among seasons and colonies (Fig. 8, Fig. S 5) and as  
509 a consequence, the  $\text{ToE}_{\text{pop}}$  varies among colonies. The ToE in sea ice and populations  
510 are earlier for colonies in East Antarctica, than in the Ross, Bellingshausen, Amundsen  
511 and Weddell Seas (Fig. S 7). The variability and trend are negatively related (Fig. S 6), so  
512 regions showing a larger signal also exhibit larger variability in climate and population as  
513 sea ice loss are projected into the future. When the environmental stochasticity generated  
514 by other factors than sea ice ( $\text{var}(\epsilon)$ ) is ignored, the  $\text{ToE}_{\text{pop}}$  occurs earlier than climate for  
515 most colonies, except the ones located from Enderby Land to Terre Adelie Land in East  
516 Antarctica for which the ToE in sea ice is the earliest. When parameter uncertainty and  
517 process variance are included, the  $\text{ToE}_{\text{pop}}$  occurs later than  $\text{ToE}_{\text{climate}}$  for almost all colonies,  
518 except the few colonies in the Bellingshausen and Amundsen Seas for sea ice during the  
519 rearing season.

## 520 **6 Discussion**

521 Anthropogenic climate change has triggered impacts on ecosystems world-wide, yet  
522 the timing at which these biological impacts can be formal detected has been insufficiently  
523 described [Beaumont *et al.*, 2011]. Here we focused on detecting climate-driven signals in  
524 population, but this approach can be applied to climate-related impacts on changes in

525 distribution by accounting for the temporal dynamics in those spatial changes. Hereto-  
526 fore, changes in distribution are often assumed to depend only on the climate signal and  
527 analyses using, for example, species distribution models often ignore climate variability  
528 (but see Zimmermann *et al.* [2009]).

529 We found that the time of emergence of climate-driven signals in population dynam-  
530 ics  $ToE_{pop}$  depends on (1) the magnitude of climate change and variability and (2) life-  
531 histories and demographic processes by which climate affects the population and we pro-  
532 pose six testable predictions. In the context of detection and attribution of climate change,  
533 we find that some life histories magnify signal-to-noise ratios in climate ( $ToE_{climate}$ ), en-  
534 abling observations of populations to yield earlier detection of anthropogenic climate  
535 change than observations of a climate variable itself— while other demographic dynam-  
536 ics prolong the detection of anthropogenic climate change relative to  $ToE_{climate}$ .

537 In our emperor penguin example, density dependent processes occur because of sex-  
538 biased mortality in response to sea ice, which displays spatiotemporal autocorrelation,  
539 affecting reproduction and survival. These dynamics result in complex co-variations  
540 among demographic rates, and the life cycle is structured in several stages. Our main  
541 theoretical result – some life histories enable an earlier  $ToE_{pop}$  than  $ToE_{climate}$ – is well sup-  
542 ported by our example when the noise is driven by climate natural variability and all  
543 complexities arising in natural systems discussed in the following sections are included.

544 However, when stochastic variations from observation error and other biotic and abi-  
545 otic processes other than sea ice natural variability are included, the  $ToE_{pop}$  occurs later  
546 than  $ToE_{climate}$  for almost all colonies. However, sampling and process errors can be re-  
547 duced by increasing monitoring effort and improving our understanding of how the bi-  
548 ological systems respond to biotic and abiotic factors. Furthermore, aggregating abun-  
549 dance across space attenuates the random component of the underlying growth rates  
550 and may permit a better detection of anthropogenic signals in populations [Che-Castaldo  
551 *et al.*, 2017].

552       Regardless of whether the stochastic noise associated with other sources than nat-  
553 ural variability in climate occludes an earlier  $ToE_{pop}$  than  $ToE_{climate}$ , the time of emer-  
554 gence identifies when the signal of anthropogenic climate change in populations can be  
555 quantitatively distinguished from year-specific stochastic variation. Quantifying  $ToE_{pop}$  is  
556 critically needed to provide relevant cost/benefit evaluations for climate mitigation and  
557 adaptation strategies, as well as accurate assessments of the risks climate change poses  
558 to conservation and management of ecosystems [Hawkins *et al.*, 2020; Hawkins & Sutton,  
559 2012]. In this context, we propose a road map for future research.

### 560 **6.1 $ToE_{pop}$ is predicted from $ToE_{climate}$**

561       We find that the  $ToE_{pop}$  depends almost linearly on the  $ToE_{climate}$  (Fig. 3). Hence, we  
562 suggest the following hypotheses.

563       [H1] *Tropical species may permit an earlier detection of anthropogenic climate change than*  
564 *temperate species, especially if temperature in summer affects their demographic rates.* Many cli-  
565 mate studies have shown that the ToE in temperature is earlier for low latitude regions  
566 than for mid-latitude regions and is of intermediate duration for polar regions [Hawkins  
567 *et al.*, 2020; Hawkins & Sutton, 2012; Mahlstein *et al.*, 2012, 2011]. The emergence of signal  
568 of anthropogenic climate warming occurs the soonest in the summer season at low lati-  
569 tudes [Mahlstein *et al.*, 2011]. The studies of Beaumont *et al.* [2011] and Sorte *et al.* [2019]  
570 support this hypothesis: tropical and subtropical ecosystems, and mangroves, face ex-  
571 treme conditions earliest than boreal forests and tundra biomes because the low SD com-  
572 pensate for the relatively small absolute changes [Beaumont *et al.*, 2011]. Passerine bird  
573 species that migrate between temperate breeding grounds in North America and south-  
574 ern tropical wintering grounds experience an earlier  $ToE_{climate}$  than species wintering in  
575 the subtropics [Sorte *et al.*, 2019].  $ToE_{climate}$  exceeding 2300 occurred only in the northern  
576 latitudes corresponding to the southern non-breeding grounds of some birds [Sorte *et al.*,  
577 2019]. Studies on the thermal tolerance of terrestrial ectotherms also support this hypoth-  
578 esis. For example, tropical insects are relatively sensitive to temperature change and are

579 currently living very close to their optimal temperature, while species at higher latitudes  
580 have broader thermal tolerance and are living in climates that are currently cooler than  
581 their physiological optima [Deutsch *et al.*, 2008].

582 [H2] *In terrestrial systems, species affected by temperature may yield earlier detection of an-*  
583 *thropogenic climate change than species affected by precipitation.* Climate studies have shown  
584 that changes in precipitation are often harder to detect because natural variability in pre-  
585 cipitation is larger than in temperature [Giorgi & Bi, 2009]. For example, the  $ToE_{climate}$  in  
586 precipitation extremes does not occur prior to 2100 in many regions [King *et al.*, 2015].  
587 However, an anthropogenic signal is emerging soon in wintertime heavy precipitation  
588 events over much of Eurasia and North America, so species in these regions may ex-  
589 perience earlier  $ToE_{pop}$ . However, this hypothesis depends also on the sensitivity of the  
590 population growth rate to temperature versus precipitation. In a comparative study of  
591 time series of 165 plants populations around the globe, Compagnoni *et al.* [2021] found  
592 that demographic responses to climate are larger for precipitation than temperature, but  
593 large noise hampers the detection of the impact of precipitation on plant populations.

594 [H3] *In marine systems, species dependent on the upper ocean biological cycling of carbon,*  
595 *photosynthetic activity, or salinity may yield later detection of anthropogenic climate change than*  
596 *species affected by sea surface temperature or pH.* Several studies found that variables inte-  
597 grating the effect of invading anthropogenic carbon into the global ocean (e.g. pH) and  
598 sea surface temperature emerged most rapidly while variables related to the upper ocean  
599 mixing, associated changes in biological processes (e.g. export of organic matter, pri-  
600 mary productivity) and salinity, only emerge after several decades [Henson *et al.*, 2017;  
601 Schlunegger *et al.*, 2020].

## 602 **6.2 ToE in population is predicted from life histories and demographic processes**

603 The  $ToE_{pop}$  can be also predicted by life histories and demographic processes that will  
604 interact with our previous three hypotheses based on the relationships between  $ToE_{pop}$   
605 and  $ToE_{climate}$  .

606 [H4]  $ToE_{pop}$  occurs later in semelparous species. Semelparous species, such as salmon,  
607 bamboos, and monocarpic herbs, exhibit a “big-bang reproduction” whereby individu-  
608 als die immediately after the first reproduction [e.g. Metcalf *et al.*, 2003]. As a conse-  
609 quence, their population dynamics is often more variable than population of iteroparous  
610 species. Indeed, the various reproductive events of iteroparous species may be spread  
611 out throughout their life as a bet-hedging strategy in unpredictable environments, buffer-  
612 ing the effect of environmental variability on population growth rate [Hilde *et al.*, 2020].  
613 However, there is little theory available to predict how the degree of iteroparity might in-  
614 fluence the demographic response to climate. A comparative study found no correlation  
615 between the degree of iteroparity with population responses to climate in plants [Com-  
616 pagnoni *et al.*, 2021]. Further work should entail a direct comparison of the influence of  
617 the generation time and degree of iteroparity on  $ToE_{pop}$ .

618 [H5] The  $ToE_{pop}$  of iteroparous species depends on the sensitivity of the population growth  
619 rate to the demographic parameter affected by climate (Fig. 5). For population dynamics that  
620 are mainly affected by the impact of climate on adult survival during the non-breeding  
621 season (‘tub’ hypothesis, Sæther *et al.* [2004]), the  $ToE_{pop}$  will occur earlier in long lived  
622 species than short lived species. This might be the case for many migratory species, when  
623 the climate conditions affects survival during the migration, and in the non breeding  
624 quarters [Sorte *et al.*, 2019]. The ‘tap’ hypothesis [Sæther *et al.*, 2004] proposes that en-  
625 vironmental conditions during the breeding season affect population size the following  
626 year because it influences the inflow of new recruits into the population. The  $ToE_{pop}$  in  
627 population occurs earlier if climate conditions during the breeding season have carry-  
628 over effect on demographic rates influencing the number of recruits, as observed in many  
629 species [e.g. Szostek & Becker, 2015]. Specifically, this will occur when climate affects  
630 juvenile survival for short lived species and maturation rate for long lived species. Ob-  
631 viously, the underlying processes of the ‘tub- tap’ effects are not mutually exclusive, and  
632 multiple demographic rates are affected by climate, that will eventually shorten or pro-

633 long the  $ToE_{pop}$ .

634 [H6] *Iteroparous species can act as earlier indicators of the detection of anthropogenic cli-*  
635 *mate change than climate itself.* Earlier  $ToE_{pop}$  than  $ToE_{climate}$  occurs when climate affects  
636 the demographic rates that most influence the population growth rate: adult survival  
637 and maturity for long-lived iteroparous species and juvenile survival for short-lived ones  
638 (Fig. 3, Fig. 5). This hypothesis is supported by our empirical example: the popula-  
639 tion growth rate is mostly sensitive to the adult survival [Jenouvrier *et al.*, 2010], which  
640 is affected by sea ice conditions [Jenouvrier *et al.*, 2012]. Here, we found that the  $ToE_{pop}$   
641 occurs earlier than  $ToE_{climate}$  when process variance due to other environmental factors  
642 and demographic parameter uncertainties is ignored (Fig. 8a). In natural system, the  
643 process variance may be large, obscuring an earlier detection of anthropogenic climate  
644 change in populations than in climate variables itself (Fig. 8b, Sæther *et al.* [2007, 2004]).  
645 However, if the goal is to use earlier indicator species in the detection of anthropogenic  
646 climate change, it is possible to reduce the demographic parameter uncertainties with  
647 higher sampling effort and decrease the process variance by a better understanding of  
648 the factors affecting the demographic processes.

### 649 **6.3 Road map for the future**

650 We provide the first theoretical study of the  $ToE_{pop}$  to understand the proximate mech-  
651 anisms of the impact of climate change and variability and demographic processes using  
652 a simple model. We illustrate how to use a climate explicit population model to quan-  
653 tify  $ToE_{pop}$  for emperor penguin, and argue that climate-dependent demographic mod-  
654 els could be developed for several species allowing future comparative analysis. But  
655 many questions remained unanswered about the effect of more complex climate-driven  
656 demographic processes occurring in natural systems such as density dependence, auto-  
657 correlation in climate, co-variation among demographic rates, population structure, and  
658 multiple climate drivers, to name a few. We propose a road map for future research, and  
659 acknowledge that we only scratched the surface on these important topics.

### 6.3.1 Comparative studies of the ToE in population using climate explicit population models

Characterizing the time of emergence requires long-term time series to define the historical unperturbed state. For many species, the unperturbed state benchmark is not available as most long-term ecological times series cover only recent decades while profound global changes were already underway. It is challenging to characterize ToE from observations in natural systems using statistical approaches, even in climate sciences. Hence, most the climate studies have used climate outputs from atmospheric–oceanic global circulation models (AOGCMs) to quantify the  $ToE_{climate}$  [Hawkins *et al.*, 2020; Hawkins & Sutton, 2012]. Similarly, we propose to develop climate explicit population models to characterize the ToE in population. We have illustrated our approach using a simple structured population matrix model [Caswell, 2001], but other demographic, trait-based or eco-evolutionary modeling frameworks can be developed.

We argue that the  $ToE_{pop}$  can be quantified for many species already [Doak & Morris, 2010; Saether *et al.*, 2019; Treurnicht *et al.*, 2016] allowing comparative studies to address our specific hypotheses on the variations of  $ToE_{pop}$  across regions, ecosystems drivers, and species life histories. In recent decades, there is an increase in the number of studies measuring the effect of climate accounting for multiple seasonal and carry-over effects of climate on the complete life cycle of a species [Cordes *et al.*, 2020; Doak & Morris, 2010; Iles & Jenouvrier, 2019; Jenouvrier, 2013; Ozgul *et al.*, 2010]. Although fewer studies have developed climate-dependent population model, the information is available in the literature to integrate the statistical relationships between climate and demographic rates into population models. The last step requires an interdisciplinary approach to use climate-dependent population models with projections of historical and future climate from AOGCMs [Iles & Jenouvrier, 2019; Jenouvrier, 2013]. AOGCMs project (often non-linear) changes in climate over time, and critically, provide quantitative estimates of natural climate variability [Kay *et al.*, 2015]. We hope that ecologists will take advantage of

687 the free availability of climate outputs in both the pre-industrial, historical and future en-  
688 vironment supervised by the Coupled Model Intercomparison Project (section 5.2). The  
689 most recently completed phase of the project (CMIP6) includes more climate models and  
690 output variables than previous phases, and importantly, includes several large ensemble  
691 runs of the same AOGCMs and experiment to account for natural variability in climate  
692 models [Deser *et al.*, 2020].

693 Finally, the key to quantifying  $ToE_{pop}$  is to characterize the population variability in  
694 the historical stationary environment. This requires careful consideration of the demo-  
695 graphic stochasticity, especially for small populations, environmental stochasticity not  
696 driven by climate, density dependence and interactions with other species, which can be  
697 incorporated in demographic models [Lande *et al.*, 2003]. Other important environmen-  
698 tal drivers of population dynamics such as habitat quality and resource variability can  
699 be incorporated into demographic models to reduce the process variance in the historical  
700 environment, enabling an earlier detection of the impact of climate change on popula-  
701 tions. This is particularly important as habitat loss and resources exploitation (land-use  
702 change, fisheries and deforestation) are key threatening processes driving the global loss  
703 in biodiversity that have synergistic effects with climate change [Dobson *et al.*, 2021; Lem-  
704 mer *et al.*, 2021; Mantyka-pringle *et al.*, 2012]. If the combined effects of those threats and  
705 climate change are greater than the effects of each threat individually, the climate driven  
706 trend in population maybe larger than the climate driven trend without interaction with  
707 other threats, with potentially earlier detection of anthropogenic forced change in popu-  
708 lations. On the other hand, if those threats augment noise in the system, that may reduce  
709 the signal to noise ratio and delay the detection of anthropogenic climate change relative  
710 to  $ToE_{climate}$ . For example, the effects of fragmentation and loss of important habitat types  
711 will reduce population size and increase the impact of demographic stochasticity on the  
712 population dynamics [Hanski & Gaggiotti, 2004; Lande, 1998], which reduces the power  
713 of detecting any signal of climate variation. In addition, environmentally induced fluctu-

714 ations in population size can be magnified by harvesting (harvest–interaction hypothesis)  
715 that may also prolong the  $ToE_{pop}$  [Gamelon *et al.*, 2019].

### 716 **6.3.2 Density Dependence**

717 Our population model does not include density dependence. The impact on the  $ToE_{pop}$   
718 will depend on the strength and type of the density dependence (negative density depen-  
719 dence: exact compensation, over-compensation, under-compensation, positive density  
720 dependence), the specific demographic rate that is affected by density dependence, the in-  
721 teraction between climate and density dependence and the life history of the species. For  
722 example, populations with undercompensating growth tend to respond slowly to envi-  
723 ronmental changes [Gamelon *et al.*, 2017; Hansen *et al.*, 2019], that may prolong the  $ToE_{pop}$ .  
724 For population declining in response to climate change the results should be qualitatively  
725 similar, except if Allee effects occur (a positive relationship between demographic rates  
726 and population), thereby accelerating extinction rate at low density [Courchamp *et al.*,  
727 2008, 1999]. The Allee effect will increase the magnitude of the decline of the popula-  
728 tion trend and  $ToE_{pop}$  will probably occurs earlier [Lande, 1998], but that will depend if  
729 an increase variance compensate for this larger signal. For population increasing in re-  
730 sponse to climate change, the patterns found without density dependence are more likely  
731 to change, that will depend on the emergence thresholds and carrying capacity of the  
732 population. For example, for invasive species, the emergence thresholds may be defined  
733 well below the carrying capacity of the population, hence the results would be qualita-  
734 tively the same as without density dependence. However, if the emergence thresholds  
735 are defined above the carrying capacity, the signal of anthropogenic climate change in  
736 population cannot be formally distinguished from population variability.

### 737 **6.3.3 Temporal autocorrelation in climate and demographic rates**

738 Our simulated environment does not include autocorrelation in the climate time se-  
739 ries, while most environmental variables exhibit a red noise that may increase the prob-  
740 ability of extinction of populations [Mustin *et al.*, 2013; Rescan *et al.*, 2020]. Environmen-

741 tal variables in reddened environments imply consecutive periods of favourable or un-  
742 favourable conditions (positive autocorrelation), and a lower probability of at least one  
743 extremely poor year compared with white noise for a given time period, which may both  
744 decrease or increase population extinction risk [Schwager *et al.*, 2006]. The response of  
745 species to coloured environmental variations depends on the time-scale considered, the  
746 strength of environmental fluctuations, the particular life-history traits that are affected  
747 by environmental change and the species life cycle defining the sensitivity of popula-  
748 tion dynamics to these fluctuations [Engen *et al.*, 2013]. For example, a study from 454  
749 plant and animal populations found that fast life histories show highest sensitivities to  
750 temporal autocorrelation in demographic rates across reproductive strategies, while slow  
751 life histories are less sensitive to temporal autocorrelation, but their sensitivities increase  
752 for species with a large degree of iteroparity [Paniw *et al.*, 2017]. An important question  
753 is then how the sensitivities to temporal autocorrelation in demographic rates is related  
754 to the  $ToE_{pop}$ , and can be addressed by incorporating such autocorrelation in our current  
755 framework. Since the patterns of the sensitivities of the population growth rate to both in-  
756 terannual variability and temporal autocorrelation in demographic rates are similar [Iles  
757 *et al.*, 2019; Paniw *et al.*, 2017], and the influence of autocorrelations on the population  
758 variability driven by environmental noise is small [Engen *et al.*, 2013], we do not expect  
759 that including temporal autocorrelation will change our six hypothesis.

#### 760 **6.3.4 Correlation among demographic rates**

761 Correlations among demographic rates can occur when climate affects rates simulta-  
762 neously, and were ignored in our simulations. Positive covariation and autocorrelation  
763 in demographic rates tend to increase the variability in demographic rates, decreasing  
764 the stochastic growth rate and increasing the variability in population growth rates [En-  
765 gen *et al.*, 2013; Tuljapurkar *et al.*, 2009]. On the opposite, negative covariation and auto-  
766 correlation tends to decrease the variability in demographic rates, such as the survival-  
767 fecundity-trade-offs that reduces the variance in the population growth rate [Colchero

768 *et al.*, 2019; Sæther & Engen, 2015]. Correlations of opposite signs among the various de-  
769 mographic rates may cancel out the effect of each other, and the resulting effect on the  
770 population growth rate maybe small. In addition, the life-history strategy and density  
771 dependence affect the population responses to covariation and autocorrelation in demo-  
772 graphic rates [Colchero *et al.*, 2019; Iles *et al.*, 2019] making challenging to predict how  
773 the trend and variability in population, hence the  $ToE_{pop}$ , will be affected by covariation  
774 among demographic rates. Demographic rate correlations had the largest effect on the  
775 population growth rate for life histories with short to medium generation time [Iles *et al.*,  
776 2019], that may amplify or dampen the detection of anthropogenic climate change.

### 777 6.3.5 Population structure

778 Our population model includes the simplest age-structure by aggregating age-classes  
779 into two stages: juvenile and adult. Although this simple life cycle is useful to explore a  
780 wide range of life histories (Table 1), it leads to a reduced variance in annual population  
781 growth rates in an unperturbed environment [Colchero *et al.*, 2019]. In our definition,  
782 the  $ToE_{pop}$  is based on the comparison of the variability between the unperturbed and  
783 perturbed environment. Hence, the resulting  $ToE_{pop}$  should not be highly sensible to  
784 the structure of the population, except if the life cycle structure buffers or amplifies the  
785 population variability response to population structure in a non-stationary environment.

786 The life cycle of many species are much more complex than our simulated life histo-  
787 ries. For example, the life cycles of plants include cryptic life stages such as long-term  
788 seedbanks and dormant adults. The reproduction of plants is highly variable with some  
789 plants reproducing vegetatively and seed mass and per-capita seed production ranging  
790 typically across six orders of magnitude [Kattge *et al.*, 2011]. Plants exhibits also an in-  
791 credible range of longevity, from weeks to millennia [Peñuelas & Munné-Bosch, 2010].  
792 For example, an alpine carex, *Carex curvula* is a very slow-growing rhizomatous sedge  
793 can have a lifespan of 2000 years [Steinger *et al.*, 1996]. The range of temperature vari-  
794 ations that this alpine flora can sustain (i.e. breath of thermal niche) is exceeding the

795 worst climate warming scenarios [Körner & Hiltbrunner, 2021], suggesting that the time  
796 of emergence would be prolonged for those species. Those complex life-history traits are  
797 not exclusive to the plant kingdom, and further work focusing on how age, stage and  
798 trait structure affect the dynamics of populations and potentially dampen or amplify the  
799 climate-driven variability in population (e.g. cohort resonance, Bjørnstad *et al.* [2004]),  
800 will provide fundamental insights to theoretical and applied research of the detection of  
801 anthropogenic climate change. For example, Bjørnstad *et al.* [2004] showed that spectral  
802 frequencies of the catches of cod in the Skagerrak were not the dominant frequencies of  
803 key environmental drivers, rather there was a spectral shift with a frequency peak at cod  
804 generational time scales, the so-called cohort resonance. Population dynamics may also  
805 potentially retain a memory of prior forcing, especially when climate events occurring in  
806 one season or stage of the life cycle affect individual performance in a subsequent sea-  
807 son or stage (e.g. carry-over effects of climate; effect of climate at young age classes that  
808 may delay age at first recruitment [Hollowed & Sundby, 2014; Lindström & Kokko, 2002;  
809 Ranta *et al.*, 2005]; effect of climate on dormant stages [Hairston Jr, 1996]).

### 810 **6.3.6 Multiple climate drivers**

811 Our modeling framework includes only a single environmental time series. The cu-  
812 mulative integrations of white-noise atmospheric forcing in ecosystem drivers can gen-  
813 erate population responses that are characterized by strong transitions and prolonged  
814 apparent state changes in marine ecosystems that will affect the  $ToE_{pop}$  [Di Lorenzo &  
815 Ohman, 2013]. In addition, integrating multiple drivers to characterize the  $ToE_{pop}$  is im-  
816 portant, as different climate variables affect organisms at various seasons and stages of  
817 their life cycle, sometimes in opposite ways [Jenouvrier, 2013; Jenouvrier *et al.*, 2018]. In a  
818 butterfly species, warmer temperatures have a positive effect on the survival of eggs, pre-  
819 diapause larvae and pupae but a negative effect on the survival of overwintering larvae  
820 [Radchuk *et al.*, 2013]. Climatic conditions experienced at different stages cause complex  
821 patterns of environmental covariance among demographic rates even across generations,

822 which may either buffer or amplify the signal of anthropogenic climate change, empha-  
823 sizing the importance of considering the complete life history of individuals when pre-  
824 dicting and detecting the effect of climatic change on population dynamics [Herfindal  
825 *et al.*, 2015; Iles *et al.*, 2019; Jenouvrier, 2013].

## 826 **7 Conclusion**

827 In the current global biodiversity crisis, the development of tools to detect, quantify,  
828 and compare the signal of anthropogenic climate change is essential to understand, antic-  
829 ipate and adapt to climate change. Here, we provide a new perspective on how climate-  
830 induced changes in populations can be detected by quantifying the Time of Emergence in  
831 populations. We hope that ecologists will embrace the relevance of this concept in their  
832 attempt to understand population responses to climate change in non-stationary environ-  
833 ments and provide a robust assessment of future climate risk to inform management and  
834 policy decisions.

## 835 **Acknowledgments**

836 We thank all the field workers who participated to the emperor penguin long-term  
837 study since 1964, and the Institute Paul Emile Victor (Programme IPEV 109), and Ter-  
838 res Australes et Antarctiques Françaises for for logistical and financial support in Terre  
839 Adélie. We thank Joannie Van de Walle and Remi Fay for their comments on earlier  
840 versions of the manuscript and Arpat Ozgul, David Iles, Jimmy Garnier, Mike Neubert,  
841 Heather Lynch, and the working group on "Individual heterogeneity in animal's life histo-  
842 ries" for constructive discussions. We acknowledge the support of NASA 80NSSC20K1289  
843 to SJ, ML and MH; NSF OPP 1744794 to SJ and NSF OPP 2037561 to SJ and MH.

## 8 References

844

845

846 Allen MR, Babiker M, Chen Y, *et al.* (2018) Summary for policymakers. In: *Global Warming*  
847 *of 1.5: An IPCC Special Report on the impacts of global warming of 1.5°C above pre-industrial*  
848 *levels and related global greenhouse gas emission pathways, in the context of strengthening the*  
849 *global response to the threat of climate change, sustainable development, and efforts to eradicate*  
850 *poverty*. IPCC.

851 Barnes E, Anderson C, Ebert-Uphoff I (2018) An ai approach to determining the time of  
852 emergence of climate change. In: *Proc. 8th International Workshop on Climate Informatics:*  
853 *CI 2018*, pp. 19–22.

854 Barnhart KR, Miller CR, Overeem I, Kay JE (2016) Mapping the future expansion of arctic  
855 open water. *Nature Climate Change*, **6**, 280–285.

856 Barraquand F, Yoccoz NG (2013) When can environmental variability benefit population  
857 growth? counterintuitive effects of nonlinearities in vital rates. *Theoretical population*  
858 *biology*, **89**, 1–11.

859 Bauwens D, Diaz-Uriarte R (1997) Covariation of life-history traits in lacertid lizards: a  
860 comparative study. *The American Naturalist*, **149**, 91–111.

861 Beaumont LJ, Pitman A, Perkins S, Zimmermann NE, Yoccoz NG, Thuiller W (2011) Im-  
862 pacts of climate change on the world's most exceptional ecoregions. *Proceedings of the*  
863 *National Academy of Sciences*, **108**, 2306–2311.

864 Bienvenu F, Legendre S (2015) A new approach to the generation time in matrix popula-  
865 tion models. *The American Naturalist*, **185**, 834–843.

866 Bjørnstad ON, Nisbet RM, FROMENTIN JM (2004) Trends and cohort resonant effects in  
867 age-structured populations. *Journal of animal ecology*, **73**, 1157–1167.

868 Boyce M, Haridas C, Lee C, Thenceasstochasticdemographyw (2006) Demography in an

869 increasingly variable world. *Trends in Ecology & Evolution*, **21**, 141–148. doi:10.1016/j.  
870 tree.2005.11.018.

871 Callendar GS (1938) The artificial production of carbon dioxide and its influence on tem-  
872 perature. *Quarterly Journal of the Royal Meteorological Society*, **64**, 223–240.

873 Caswell H (2001) *Matrix population models*, vol. Second. Sinauer, Sunderland, Mas-  
874 sachusetts, - pp.

875 Che-Castaldo C, Jenouvrier S, Youngflesh C, *et al.* (2017) Pan-antarctic analysis aggreg-  
876 ating spatial estimates of adélie penguin abundance reveals robust dynamics despite  
877 stochastic noise. *Nature communications*, **8**, 832.

878 Colchero F, Jones OR, Conde DA, *et al.* (2019) The diversity of population responses to  
879 environmental change. *Ecology Letters*. doi:10.1111/ele.13195.

880 Compagnoni A, Levin S, Childs DZ, *et al.* (2021) Herbaceous perennial plants with short  
881 generation time have stronger responses to climate anomalies than those with longer  
882 generation time. *Nature Communications*, **12**. doi:10.1038/s41467-021-21977-9.

883 Cordes LS, Blumstein DT, Armitage KB, *et al.* (2020) Contrasting effects of climate change  
884 on seasonal survival of a hibernating mammal. *Proceedings of the National Academy of  
885 Sciences*, **117**, 18119–18126.

886 Courchamp F, Berec L, Gascoigne J (2008) *Allee effects in ecology and conservation*. Oxford  
887 University Press.

888 Courchamp F, Clutton-Brock T, Grenfell B (1999) Inverse density dependence and the  
889 allee effect. *Trends in ecology & evolution*, **14**, 405–410.

890 Deser C, Knutti R, Solomon S, Phillips AS (2012) Communication of the role of natural  
891 variability in future north american climate. *Nature Climate Change*, **2**, 775–779.

892 Deser C, Lehner F, Rodgers KB, *et al.* (2020) Insights from earth system model initial-  
893 condition large ensembles and future prospects. *Nature Climate Change*, **10**, 277–286.  
894 doi:10.1038/s41558-020-0731-2.

- 895 Deutsch CA, Tewksbury JJ, Huey RB, Sheldon KS, Ghalambor CK, Haak DC, Martin PR  
896 (2008) Impacts of climate warming on terrestrial ectotherms across latitude. *Proceedings*  
897 *of the National Academy of Sciences*, **105**, 6668–6672. doi:10.1073/pnas.0709472105.
- 898 Di Lorenzo E, Ohman MD (2013) A double-integration hypothesis to explain ocean  
899 ecosystem response to climate forcing. *Proceedings of the National Academy of Sciences*,  
900 **110**, 2496–2499.
- 901 Doak DF, Morris WF (2010) Demographic compensation and tipping points in climate-  
902 induced range shifts. *Nature*, **467**, 959–962.
- 903 Dobson A, Rowe Z, Berger J, Wholey P, Caro T (2021) Biodiversity loss due to more than  
904 climate change. *Science*, **374**, 699–700.
- 905 Engen S, Bakke Ø, Islam A (1998) Demographic and environmental stochasticity-concepts  
906 and definitions. *Biometrics*, pp. 840–846.
- 907 Engen S, Lande R, Sæther BE (2013) A quantitative genetic model of r-and k-selection in  
908 a fluctuating population. *The American Naturalist*, **181**, 725–736.
- 909 Engen S, Lande R, Sæther BE, Weimerskirch H (2005) Extinction in relation to demo-  
910 graphic and environmental stochasticity in age-structured models. *Mathematical bio-*  
911 *sciences*, **195**, 210–227.
- 912 Fretwell PT, LaRue MA, Morin P, *et al.* (2012) An Emperor Penguin Population Estimate:  
913 The First Global, Synoptic Survey of a Species from Space. *PLoS ONE*, **7**, e33751.
- 914 Fretwell PT, Trathan PN (2009) Penguins from space: faecal stains reveal the location of  
915 emperor penguin colonies. *Global Ecology and Biogeography*, **18**, 543–552. doi:10.1111/j.  
916 1466-8238.2009.00467.x.
- 917 Gaillard J, Yoccoz N (2003) Temporal variation in survival of mammals: a case of environ-  
918 mental canalization? *Ecology*, **84**, 3294–3306.
- 919 Gaillard JM, Lemaître JF, Berger V, *et al.* (2016) *Encyclopedia of Evolutionary Biology.*, chap.  
920 Life Histories, Axes of Variation, p. 312–323. Oxford: Academic Press.

- 921 Gaillard JM, Mark Hewison A, Klein F, Plard F, Douhard M, Davison R, Bonenfant  
922 C (2013) How does climate change influence demographic processes of widespread  
923 species? lessons from the comparative analysis of contrasted populations of roe deer.  
924 *Ecology letters*, **16**, 48–57.
- 925 Gaillard JM, Yoccoz NG, Lebreton JD, *et al.* (2005) Generation time: a reliable metric to  
926 measure life-history variation among mammalian populations. *The American Naturalist*,  
927 **166**, 119–123.
- 928 Gamelon M, Grøtan V, Nilsson AL, *et al.* (2017) Interactions between demography and  
929 environmental effects are important determinants of population dynamics. *Science Ad-*  
930 *vances*, **3**, e1602298.
- 931 Gamelon M, Sandercock BK, Sæther BE (2019) Does harvesting amplify environmentally  
932 induced population fluctuations over time in marine and terrestrial species? *Journal of*  
933 *Applied Ecology*, **56**, 2186–2194.
- 934 Ghil M (2002) Natural climate variability. *Encyclopedia of global environmental change*, **1**,  
935 544–549.
- 936 Giorgi F, Bi X (2009) Time of emergence (TOE) of GHG-forced precipitation change hot-  
937 spots. *Geophysical Research Letters*, **36**. doi:10.1029/2009gl037593.
- 938 Hairston Jr NG (1996) Zooplankton egg banks as biotic reservoirs in changing environ-  
939 ments. *Limnology and Oceanography*, **41**, 1087–1092.
- 940 Hansen BB, Gamelon M, Albon SD, *et al.* (2019) More frequent extreme climate events  
941 stabilize reindeer population dynamics. *Nature communications*, **10**, 1–8.
- 942 Hanski IA, Gaggiotti OE (2004) *Ecology, genetics and evolution of metapopulations*. Academic  
943 Press.
- 944 Hasselmann K (1976) Stochastic climate models part i. theory. *tellus*, **28**, 473–485.
- 945 Hawkins E, Frame D, Harrington L, Joshi M, King A, Rojas M, Sutton R (2020) Observed  
946 emergence of the climate change signal: From the familiar to the unknown. *Geophysical*

- 947 *Research Letters*, **47**. doi:10.1029/2019gl086259.
- 948 Hawkins E, Sutton R (2009) The potential to narrow uncertainty in regional climate pre-  
949 dictions. *Bulletin of the American Meteorological Society*, **90**, 1095–1108.
- 950 Hawkins E, Sutton R (2012) Time of emergence of climate signals. *Geophysical Research*  
951 *Letters*, **39**, n/a–n/a. doi:10.1029/2011gl050087.
- 952 Henson SA, Beaulieu C, Ilyina T, *et al.* (2017) Rapid emergence of climate change in en-  
953 vironmental drivers of marine ecosystems. *Nature Communications*, **8**. doi:10.1038/  
954 ncomms14682.
- 955 Herfindal I, van de Pol M, Nielsen JT, Sæther BE, Møller AP (2015) Climatic conditions  
956 cause complex patterns of covariation between demographic traits in a long-lived rap-  
957 tor. *Journal of Animal Ecology*, **84**, 702–711.
- 958 Hilde CH, Gamelon M, Sæther BE, Gaillard JM, Yoccoz NG, Pélabon C (2020) The demo-  
959 graphic buffering hypothesis: evidence and challenges. *Trends in ecology & evolution*, **35**,  
960 523–538.
- 961 Hollowed AB, Sundby S (2014) Change is coming to the northern oceans. *Science*, **344**,  
962 1084–1085.
- 963 Iles D, Jenouvrier S (2019) *Projected population consequences of climate change*, pp. 147–164.  
964 Oxford University Press.
- 965 Iles DT, Rockwell RF, Koons DN (2019) Shifting vital rate correlations alter predicted pop-  
966 ulation responses to increasingly variable environments. *The American Naturalist*, **193**,  
967 E57–E64. doi:10.1086/701043.
- 968 Jenouvrier S (2013) Impacts of climate change on avian populations. *Global Change Biology*,  
969 **19**, 2036–2057.
- 970 Jenouvrier S, Barbraud C, Weimerskirch H (2005) Long-term contrasted responses to cli-  
971 mate of two antarctic seabirds species. *Ecology*, **86**, 2889–2903.
- 972 Jenouvrier S, Caswell H, Barbraud C, Weimerskirch H (2010) Mating behavior, popula-

973 tion growth, and the operational sex ratio: A periodic two-sex model approach. *The*  
974 *American naturalist*, **175**, 739–752. doi:10.1086/652436.

975 Jenouvrier S, Desprez M, Fay R, Barbraud C, Weimerskirch H, Delord K, Caswell H (2018)  
976 Climate change and functional traits affect population dynamics of a long-lived seabird.  
977 *Journal of Animal Ecology*, **87**, 906–920.

978 Jenouvrier S, Garnier J, Patout F, Desvillettes L (2017) Influence of dispersal processes  
979 on the global dynamics of emperor penguin, a species threatened by climate change.  
980 *Biological Conservation*, **212**, 63–73.

981 Jenouvrier S, Holland M, Iles D, *et al.* (2020) The paris agreement objectives will likely halt  
982 future declines of emperor penguins. *Global change biology*, **26**, 1170–1184.

983 Jenouvrier S, Holland M, Stroeve J, Barbraud C, Weimerskirch H, Serreze M, Caswell H  
984 (2012) Effects of climate change on an emperor penguin population: analysis of coupled  
985 demographic and climate models. *Global Change Biology*, **18**, 2756–2770. doi:10.1111/j.  
986 1365-2486.2012.02744.x.

987 Jenouvrier S, Holland M, Stroeve J, Serreze M, Barbraud C, Weimerskirch H, Caswell H  
988 (2014) Projected continent-wide declines of the emperor penguin under climate change.  
989 *Nature Climate Change*, **4**, 715.

990 Jenouvrier S, Judy CC, Wolf S, *et al.* (2021) The call of the emperor penguin: Legal re-  
991 sponses to species threatened by climate change. *Global Change Biology*.

992 Kattge J, Diaz S, Lavorel S, *et al.* (2011) Try—a global database of plant traits. *Global change*  
993 *biology*, **17**, 2905–2935.

994 Kay J, Deser C, Phillips A, *et al.* (2015) The community earth system model (cesm) large  
995 ensemble project: A community resource for studying climate change in the presence of  
996 internal climate variability. *Bulletin of the American Meteorological Society*, **96**, 1333–1349.

997 King AD, Donat MG, Fischer EM, *et al.* (2015) The timing of anthropogenic emergence in  
998 simulated climate extremes. *Environmental Research Letters*, **10**, 094015.

- 999 Kooyman G, Ainley D, Ballard G, Ponganis P (2007) Effects of giant icebergs on two em-  
1000 peror penguin colonies in the ross sea, antarctica. *Antarctic Science*, **19**, 31–38.
- 1001 Körner C, Hiltbrunner E (2021) Why is the alpine flora comparatively robust against cli-  
1002 matic warming? *Diversity*, **13**, 383.
- 1003 Lande R (1998) Anthropogenic, ecological and genetic factors in extinction and conserva-  
1004 tion. *Population Ecology*, **40**, 259–269.
- 1005 Lande R, Engen S, Saether B (2003) *Stochastic Population Dynamics in Ecology and Conserva-*  
1006 *tion*. Oxford University Press.
- 1007 Landrum L, Holland MM (2020) Extremes become routine in an emerging new arctic.  
1008 *Nature Climate Change*, **10**, 1108–1115.
- 1009 Lemmer J, Andrzejak M, Compagnoni A, Knight TM, Korell L (2021) Climate change  
1010 and grassland management interactively influence the population dynamics of bromus  
1011 erectus (poaceae). *Basic and Applied Ecology*, **56**, 226–238.
- 1012 Lindström J, Kokko H (2002) Cohort effects and population dynamics. *Ecology Letters*, **5**,  
1013 338–344.
- 1014 Long MC, Deutsch C, Ito T (2016) Finding forced trends in oceanic oxygen. *Global Biogeo-*  
1015 *chemical Cycles*, **30**, 381–397.
- 1016 Lyu K, Zhang X, Church JA, Slangen AB, Hu J (2014) Time of emergence for regional  
1017 sea-level change. *Nature Climate Change*, **4**, 1006–1010.
- 1018 Mahlstein I, Daniel JS, Solomon S (2013) Pace of shifts in climate regions increases with  
1019 global temperature. *Nature Climate Change*, **3**, 739–743. doi:10.1038/nclimate1876.
- 1020 Mahlstein I, Hegerl G, Solomon S (2012) Emerging local warming signals in observational  
1021 data. *Geophysical Research Letters*, **39**, n/a–n/a. doi:10.1029/2012gl053952.
- 1022 Mahlstein I, Knutti R, Solomon S, Portmann RW (2011) Early onset of significant local  
1023 warming in low latitude countries. *Environmental Research Letters*, **6**, 034009.
- 1024 Mann ME, Steinman BA, Brouillette DJ, Miller SK (2021) Multidecadal climate oscillations

1025 during the past millennium driven by volcanic forcing. *Science*, **371**, 1014–1019.

1026 Mantyka-pringle CS, Martin TG, Rhodes JR (2012) Interactions between climate and habi-  
1027 tat loss effects on biodiversity: a systematic review and meta-analysis. *Global Change*  
1028 *Biology*, **18**, 1239–1252.

1029 Mason LR, Green RE, Howard C, *et al.* (2019) Population responses of bird populations  
1030 to climate change on two continents vary with species' ecological traits but not with  
1031 direction of change in climate suitability. *Climatic Change*, **157**, 337–354. doi:10.1007/  
1032 s10584-019-02549-9.

1033 Meinshausen M, Smith SJ, Calvin K, *et al.* (2011) The rcp greenhouse gas concentrations  
1034 and their extensions from 1765 to 2300. *Climatic change*, **109**, 213–241.

1035 Metcalf JC, Rose KE, Rees M (2003) Evolutionary demography of monocarpic perennials.  
1036 *Trends in Ecology & Evolution*, **18**, 471–480.

1037 Mora C, Frazier AG, Longman RJ, *et al.* (2013) The projected timing of climate departure  
1038 from recent variability. *Nature*, **502**, 183–187.

1039 Morris W, Pfister C, Tuljapurkar S, *et al.* (2008) Longevity can buffer plant and animal  
1040 populations against changing climate variability. *ecology*, **89**, 19–25.

1041 Mustin K, Dytham C, Benton TG, Travis JMJ (2013) Red noise increases extinction risk  
1042 during rapid climate change. *Diversity and Distributions*, **19**, 815–824. doi:10.1111/ddi.  
1043 12038.

1044 Neubert M, Caswell H (2000) Density-dependent vital rates and their population dynamic  
1045 consequences. *J Math Biol*, **41**, 103–121.

1046 Oli MK (2004) The fast–slow continuum and mammalian life-history patterns: an empir-  
1047 ical evaluation. *Basic and Applied Ecology*, **5**, 449–463.

1048 O'Neill BC, Tebaldi C, Vuuren DPv, *et al.* (2016) The scenario model intercomparison  
1049 project (scenariomip) for cmip6. *Geoscientific Model Development*, **9**, 3461–3482.

1050 Ozgul A, Childs DZ, Oli MK, *et al.* (2010) Coupled dynamics of body mass and population

1051 growth in response to environmental change. *Nature*, **466**, 482.

1052 Paniw M, Ozgul A, Salguero-Gómez R (2017) Interactive life-history traits predict sensi-  
1053 tivity of plants and animals to temporal autocorrelation. *Ecology Letters*, **21**, 275–286.  
1054 doi:10.1111/ele.12892.

1055 Parmesan C, Burrows MT, Duarte CM, Poloczanska ES, Richardson AJ, Schoeman DS,  
1056 Singer MC (2013) Beyond climate change attribution in conservation and ecological  
1057 research. *Ecology letters*, **16**, 58–71.

1058 Peñuelas J, Munné-Bosch S (2010) Potentially immortal? *The New Phytologist*, **187**, 564–  
1059 567.

1060 Radchuk V, Turlure C, Schtickzelle N (2013) Each life stage matters: the importance of as-  
1061 sessing the response to climate change over the complete life cycle in butterflies. *Journal*  
1062 *of Animal Ecology*, **82**, 275–285.

1063 Ranta E, Lundberg P, Kaitala V (2005) *Ecology of populations*. Cambridge University Press.

1064 Reed PB, Bridgham SD, Pfeifer-Meister LE, *et al.* (2021) Climate warming threatens the  
1065 persistence of a community of disturbance-adapted native annual plants. *Ecology*, **102**,  
1066 e03464.

1067 Rescan M, Grulois D, Ortega-Aboud E, Chevin LM (2020) Phenotypic memory drives  
1068 population growth and extinction risk in a noisy environment. *Nature ecology & evolu-*  
1069 *tion*, **4**, 193–201.

1070 Revelle R, Suess HE (1957) Carbon dioxide exchange between atmosphere and ocean and  
1071 the question of an increase of atmospheric co<sub>2</sub> during the past decades. *Tellus*, **9**, 18–27.

1072 Rojas M, Lambert F, Ramirez-Villegas J, Challinor AJ (2019) Emergence of robust pre-  
1073 cipitation changes across crop production areas in the 21st century. *Proceedings of the*  
1074 *National Academy of Sciences*, **116**, 6673–6678. doi:10.1073/pnas.1811463116.

1075 Román-Palacios C, Wiens JJ (2020) Recent responses to climate change reveal the drivers  
1076 of species extinction and survival. *Proceedings of the National Academy of Sciences*, **117**,

1077 4211–4217.

1078 Roth G, Caswell H (2018) Occupancy time in sets of states for demographic models. *The-*  
1079 *oretical Population Biology*, pp. 62–77. doi:doi:10.1016/j.tpb.2017.12.007.

1080 Saether B, Bakke O (2000) Avian life history variation and contribution of demographic  
1081 trait to the population growth rate. *Ecology*, **81**, 642–653.

1082 Sæther BE (1987) The influence of body weight on the covariation between reproductive  
1083 traits in european birds. *Oikos*, pp. 79–88.

1084 Sæther BE, Engen S (2015) The concept of fitness in fluctuating environments. *Trends in*  
1085 *ecology & evolution*, **30**, 273–281.

1086 Saether BE, Engen S, Gamelon M, Grøtan V (2019) Predicting the effects of climate change  
1087 on bird population dynamics. In: *Effects of Climate Change on Birds*, pp. 74–90. Oxford  
1088 University Press.

1089 Sæther BE, Lillegard M, Grøtan V, Filli F, Engen S (2007) Predicting fluctuations of rein-  
1090 troduced ibex populations: the importance of density dependence, environmental  
1091 stochasticity and uncertain population estimates. *Journal of Animal Ecology*, **76**, 326–336.

1092 Sæther BE, Sutherland WJ, Engen S (2004) Climate influences on avian population dy-  
1093 namics. *Advances in Ecological Research*, **35**, 185–209.

1094 Salguero-Gómez R, Jones OR, Jongejans E, *et al.* (2016) Fast–slow continuum and repro-  
1095 ductive strategies structure plant life-history variation worldwide. *Proceedings of the*  
1096 *National Academy of Sciences*, **113**, 230–235.

1097 Schlunegger S, Rodgers KB, Sarmiento JL, *et al.* (2020) Time of emergence and large en-  
1098 semble intercomparison for ocean biogeochemical trends. *Global Biogeochemical Cycles*,  
1099 **34**. doi:10.1029/2019gb006453.

1100 Schwager M, Johst K, Jeltsch F (2006) Does red noise increase or decrease extinction risk?  
1101 single extreme events versus series of unfavorable conditions. *The American Naturalist*,  
1102 **167**, 879–888.

- 1103 Schwalm CR, Glendon S, Duffy PB (2020) Rcp8. 5 tracks cumulative co2 emissions. *Pro-*  
1104 *ceedings of the National Academy of Sciences*, **117**, 19656–19657.
- 1105 Sorte FAL, Fink D, Johnston A (2019) Time of emergence of novel climates for north amer-  
1106 ican migratory bird populations. *Ecography*, **42**, 1079–1091. doi:10.1111/ecog.04408.
- 1107 Stearns SC (1983) The influence of size and phylogeny on patterns of covariation among  
1108 life-history traits in the mammals. *Oikos*, pp. 173–187.
- 1109 Steinger T, Körner C, Schmid B (1996) Long-term persistence in a changing climate: Dna  
1110 analysis suggests very old ages of clones of alpine carex curvula. *Oecologia*, **105**, 94–99.
- 1111 Stephens PA, Mason LR, Green RE, *et al.* (2016) Consistent response of bird populations  
1112 to climate change on two continents. *Science*, **352**, 84–87.
- 1113 Szostek KL, Becker PH (2015) Survival and local recruitment are driven by environmental  
1114 carry-over effects from the wintering area in a migratory seabird. *Oecologia*, **178**, 643–  
1115 657.
- 1116 Trathan PN, Wienecke B, Barbraud C, *et al.* (2020) The emperor penguin-vulnerable to  
1117 projected rates of warming and sea ice loss. *Biological Conservation*, **241**, 108216.
- 1118 Treurnicht M, Pagel J, Esler KJ, *et al.* (2016) Environmental drivers of demographic vari-  
1119 ation across the global geographical range of 26 plant species. *Journal of Ecology*, **104**,  
1120 331–342. doi:10.1111/1365-2745.12508.
- 1121 Tuljapurkar S, Gaillard JM, Coulson T (2009) From stochastic environments to life histo-  
1122 ries and back. *Philosophical Transactions of the Royal Society B: Biological Sciences*, **364**,  
1123 1499–1509. doi:10.1098/rstb.2009.0021.
- 1124 Tuljapurkar S, Orzack S (1980) Population dynamics in variable environments I. Long-run  
1125 growth rates and extinction. *Theoretical Population Biology*, **18**, 314–342.
- 1126 Tuljapurkar SD (1982) Population dynamics in variable environments. iii. evolutionary  
1127 dynamics of r-selection. *Theoretical population biology*, **21**, 141–165.
- 1128 Vázquez DP, Gianoli E, Morris WF, Bozinovic F (2015) Ecological and evolutionary im-

1129 pacts of changing climatic variability. *Biological Reviews*, **92**, 22–42. doi:10.1111/brv.  
1130 12216.

1131 Zappa G, Hoskins BJ, Shepherd TG (2015) Improving climate change detection through  
1132 optimal seasonal averaging: The case of the north atlantic jet and european precipita-  
1133 tion. *Journal of Climate*, **28**, 6381–6397.

1134 Zimmermann NE, Yoccoz NG, Edwards TC, *et al.* (2009) Climatic extremes improve pre-  
1135 dictions of spatial patterns of tree species. *Proceedings of the National Academy of Sciences*,  
1136 **106**, 19723–19728.

## 1137 **Figure**

1138 **Figure 1:** Conceptual diagram of the time of emergence (ToE) in climate ( $ToE_{climate}$ ) and  
1139 in populations ( $ToE_{pop}$ ). ToE identifies the point in time when the signal of anthropogenic  
1140 climate change (red time series) emerges from the noise associated with natural variability  
1141 (black time series).  $ToE_{pop}$  depends on the response of population growth rate to climate  
1142 that is defined by: (1) the impact of climate on demographic rates (e.g. survival) with  
1143 different functional forms that influence the sensitivity of demographic rates to climate;  
1144 (2) the impact of demographic rates on the population growth rate resulting from non-  
1145 linear demographic processes occurring throughout the species life cycle (described in  
1146 section Population projections).

1147 **Figure 2:** Illustrative figure of the time of emergence in climate ( $ToE_{climate}$  on left panel)  
1148 and in populations ( $ToE_{pop}$  on right panels) of four species along the gradient of life his-  
1149 tories, from fast species (species 1) to slow species (species 4). The figure shows one time  
1150 series simulated during the historical environment (black line) and forced environment  
1151 (red line). The emergence thresholds are based on a 95% prediction interval of 1000 sim-  
1152 ulations (grey area). The natural variability in climate is  $\sigma = 0.5$ . The forced perturbation  
1153 occurs at years 80 years resulting in a positive trend in climate. Climate affects negatively  
1154 maturation rate (slope of the linear relationship on logit scale:  $\beta = -0.125$ ). Y-axis is  
1155 different for each species.

1156 **Figure 3:** Relationship between  $ToE_{climate}$  (x-axis) and  $ToE_{pop}$  (y-axis) for four life his-  
1157 tory strategies (from fast (species 1) to slow (species 4)), whereby climate affects only one  
1158 demographic parameter at a time (colored dots: blue is fertility, red is juvenile survival,  
1159 orange is adult survival and purple is maturation rate). Black lines represent the time  
1160 when  $ToE_{pop} = ToE_{climate}$ .

1161 **Figure 4:** a) The variability in annual population growth rates depends on the natural  
1162 variability of climate  $\sigma$ , in both in the historical and perturbed environment (example for

1163  $\beta = 0.125$   $\alpha = 0.05$ ). (b) The trend of population growth rate at the time of emergence  
1164 in population depends on the trend of climate  $\alpha$  (example for  $\beta = 0.125$  and  $\sigma = 0.5$  ).  
1165 Colors refer to the climate-dependent demographic rate: blue is fertility, red is juvenile  
1166 survival, orange is adult survival and purple is maturation rate. The dots on (a) stand for  
1167 the forced environment while square are the historical environment. Panels show four  
1168 different life history strategies, from fast (species 1) to slow (species 4).

1169 **Figure 5:**  $ToE_{pop}$  as function of the sensitivity of the population growth rate to the  
1170 demographic rate affected by climate. The  $ToE_{pop}$  is the median across various natural  
1171 variability and trend of climate and various slope in the functional relationship between  
1172 climate and the demographic rate (Table 2). The sensitivity of the population growth rate  
1173 to the demographic rate is calculated for the averaged population matrix in the historical  
1174 environment. Symbols refer to species.

1175 **Figure 6:**  $ToE_{pop}$  as function of the absolute slope of the functional relationship be-  
1176 tween climate and demographic rate  $\beta_0$ . Example for a climate trend of  $\alpha = 0.05$  and  
1177 climate variability of  $\sigma = 0.5$  . Colors refer to demographic pathway by which climate af-  
1178 fects demographic rates: blue is fertility, red is juvenile survival, orange is adult survival  
1179 and purple is maturation rate. The dots stand for  $\beta_0 > 0$ , while square shows  $\beta_0 < 0$ .  
1180 Panels show four life history strategies.

1181 **Figure 7:** Annual life-cycle graph for the emperor penguin. It represents a two-sex  
1182 model with males (black) and females (gray). Fertilities are shown by dotted lines, and  
1183 the transitions between stages of individuals already present in the population are repre-  
1184 sented by solid lines (see Figure 1 from Jenouvrier *et al.* [2010] for more details on seasonal  
1185 cycle of the emperor penguin).

1186 **Figure 8:** Difference between the time of emergence in sea ice and  $ToE_{pop}$  of emperor  
1187 penguin ( $ToE_{climate} - ToE_{pop}$ ) for the 54 known colonies (x-axis) and four seasons (color).  
1188 The calculation of  $ToE_{pop}$  accounts for  $var(\epsilon)$  generated by parameter uncertainty and pro-  
1189 cess variance (i.e., environmental stochasticity) (a) or not (b).

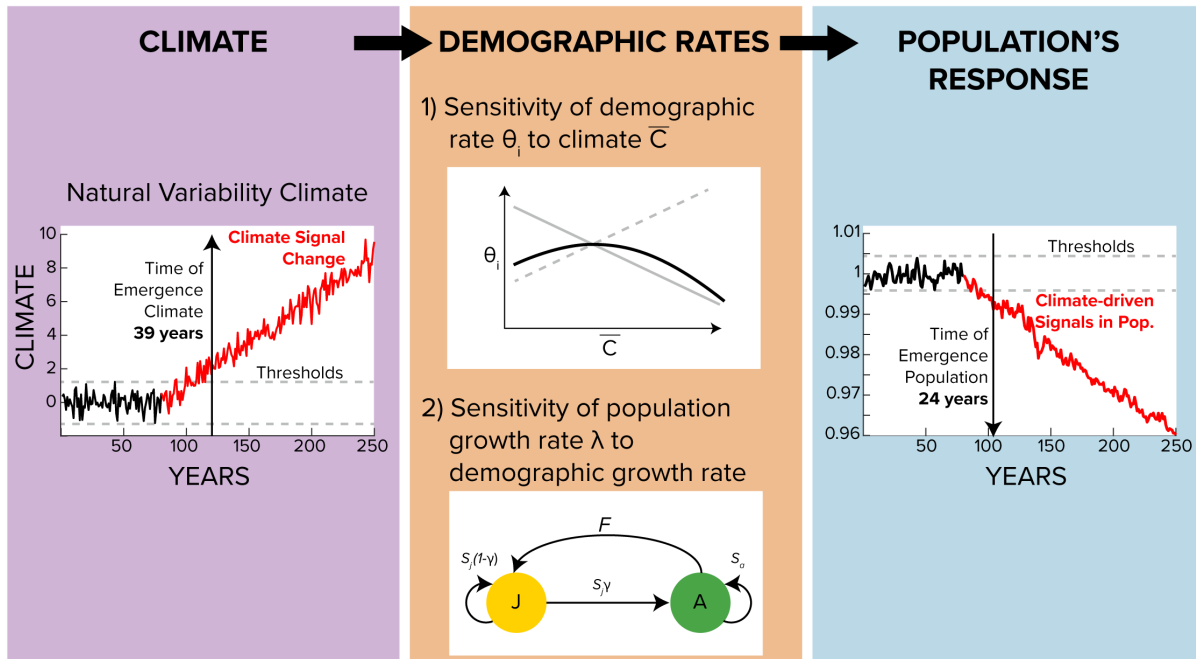


**Figure 1:** Conceptual diagram of the time of emergence (ToE) in climate ( $ToE_{climate}$ ) and in populations ( $ToE_{pop}$ ). ToE identifies the point in time when the signal of anthropogenic climate change (red time series) emerges from the noise associated with natural variability (black time series).  $ToE_{pop}$  depends on the response of population growth rate to climate that is defined by: (1) the impact of climate on demographic rates (e.g. survival) with different functional forms that influence the sensitivity of demographic rates to climate; (2) the impact of demographic rates on the population growth rate resulting from non-linear demographic processes occurring throughout the species life cycle (described in section Population projections).

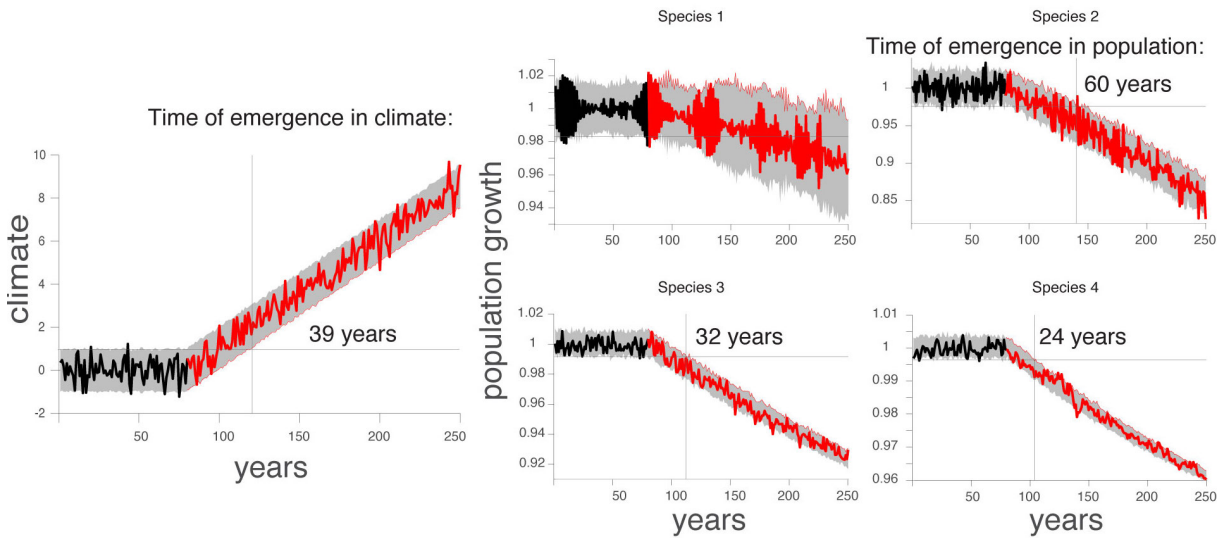


**Figure 2:** Illustrative figure of the time of emergence in climate ( $ToE_{climate}$  on left panel) and in populations ( $ToE_{pop}$  on right panels) of four species along the gradient of life histories, from fast species (species 1) to slow species (species 4). The figure shows one time series simulated during the historical environment (black line) and forced environment (red line). The emergence thresholds are based on a 95% prediction interval of 1000 simulations (grey area). The natural variability in climate is  $\sigma = 0.5$ . The forced perturbation occurs at years 80 years resulting in a positive trend in climate. Climate affects negatively maturation rate (slope of the linear relationship on logit scale:  $\beta = -0.125$ ). Y-axis is different for each species.

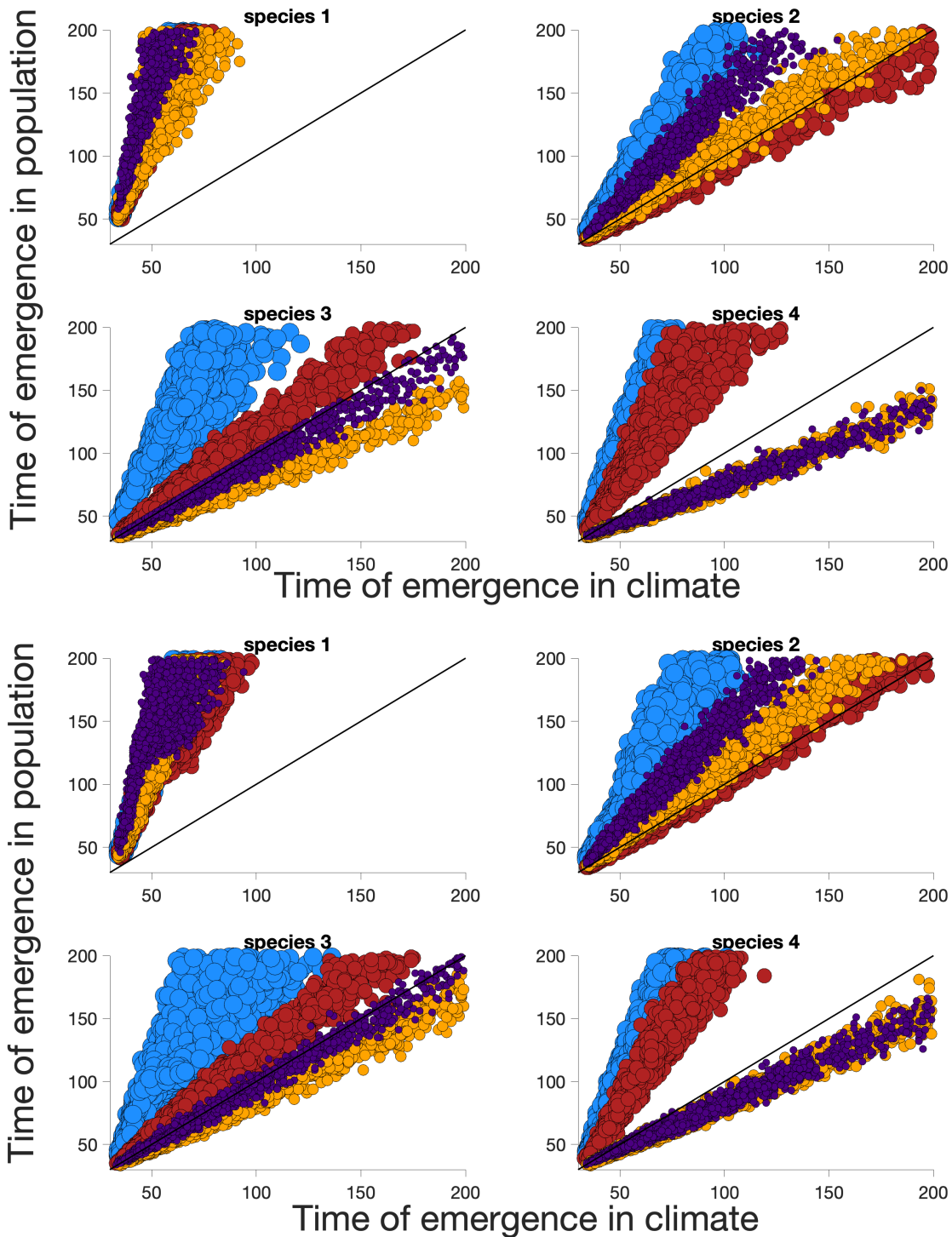


**Figure 3:** Relationship between  $ToE_{climate}$  (x-axis) and  $ToE_{pop}$  (y-axis) for four life history strategies (from fast (species 1) to slow (species 4)), whereby climate affects only one demographic parameter at a time (colored dots: blue is fertility, red is juvenile survival, orange is adult survival and purple is maturation rate). Black lines represent the time when  $ToE_{pop} = ToE_{climate}$ .

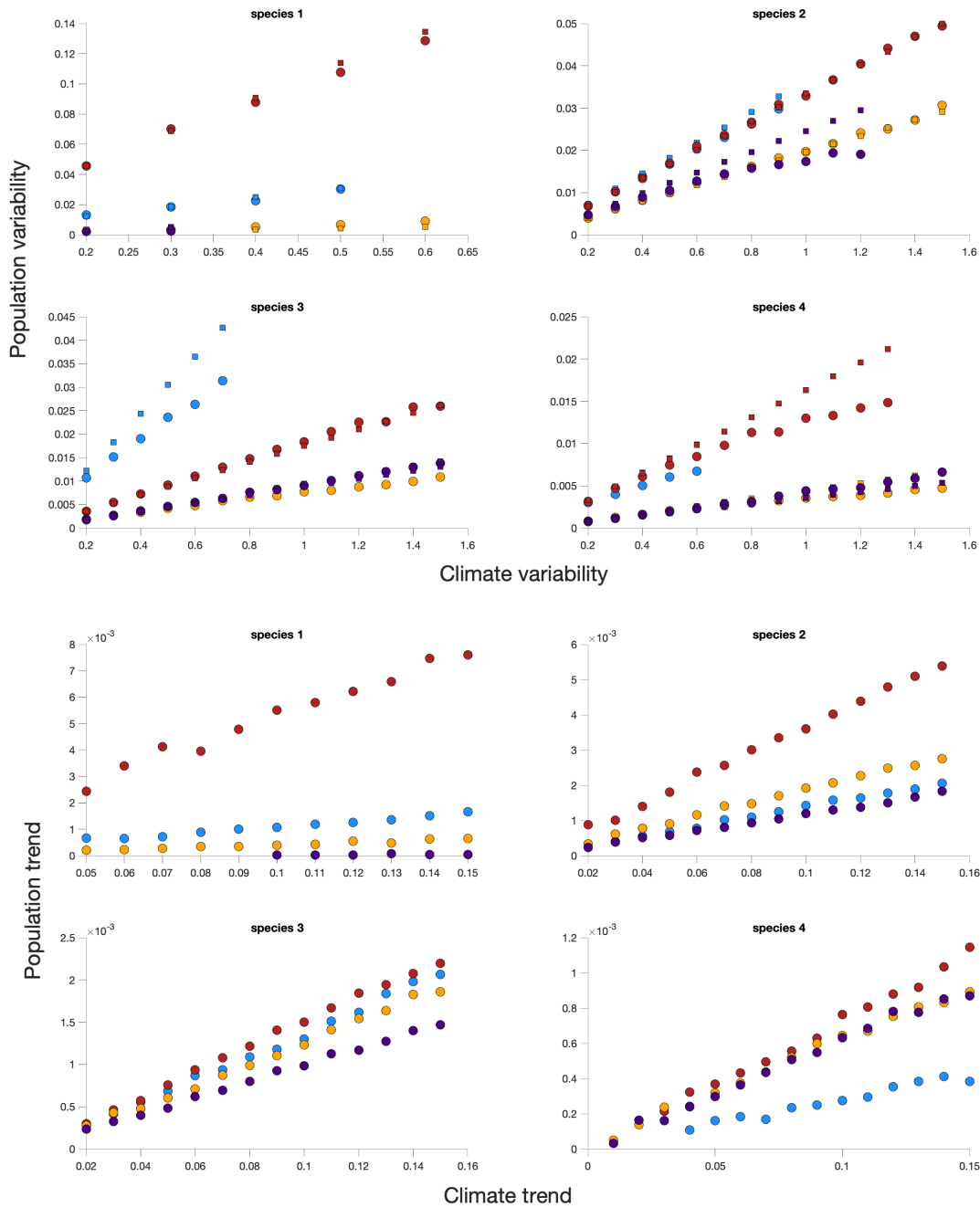


**Figure 4:** (a) The variability in annual population growth rates depends on the natural variability of climate  $\sigma$ , in both in the historical and perturbed environment (example for  $\beta = 0.125$   $\alpha = 0.05$ ). (b) The trend of population growth rate at the time of emergence in population depends on the trend of climate  $\alpha$  (example for  $\beta = 0.125$  and  $\sigma = 0.5$ ). Colors refer to the climate-dependent demographic rate: blue is fertility, red is juvenile survival, orange is adult survival and purple is maturation rate. The dots on (a) stand for the forced environment while square are the historical environment. Panels show four different life history strategies, from fast (species 1) to slow (species 4).

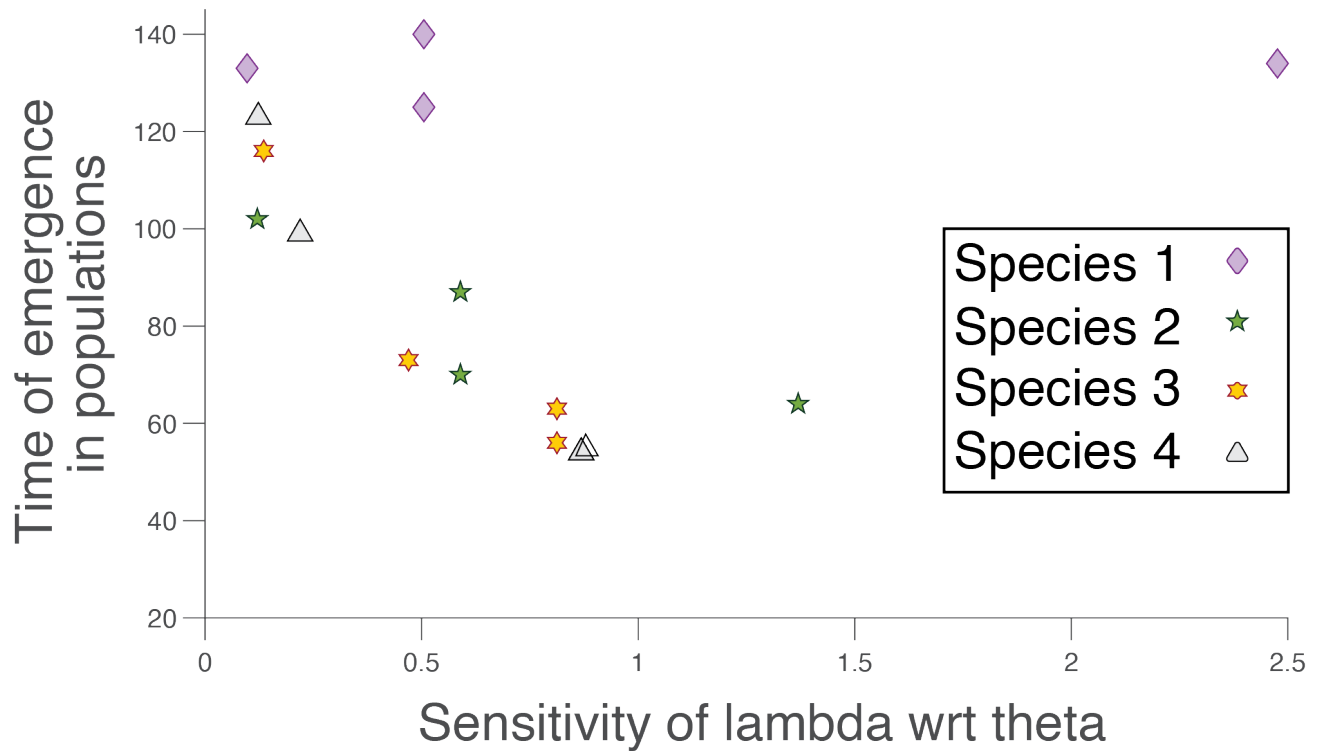


**Figure 5:**  $ToE_{pop}$  as function of the sensitivity of the population growth rate to the demographic rate affected by climate. The  $ToE_{pop}$  is the median across various natural variability and trend of climate and various slope in the functional relationship between climate and the demographic rate (Table 1). The sensitivity of the population growth rate to the demographic rate is calculated for the averaged population matrix in the historical environment. Symbols refer to species.

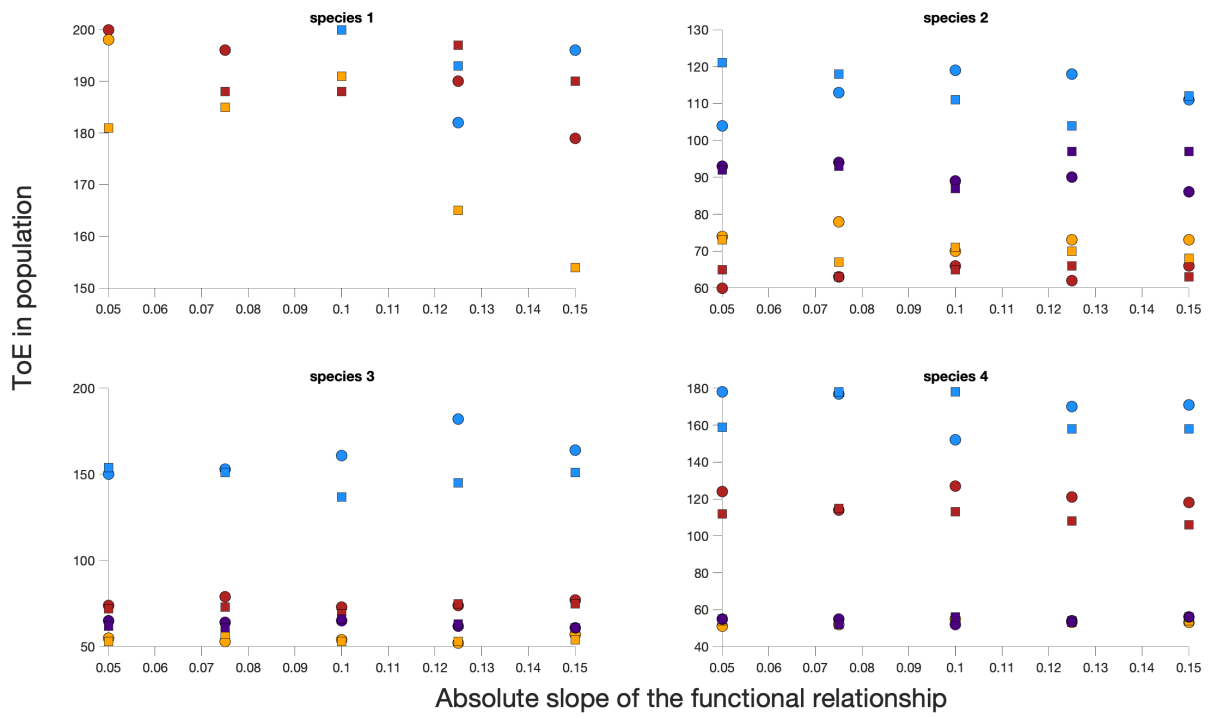


**Figure 6:**  $ToE_{pop}$  as function of the absolute slope of the functional relationship between climate and demographic rate  $\beta_0$ . Example for a climate trend of  $\alpha = 0.05$  and climate variability of  $\sigma = 0.5$ . Colors refer to demographic pathway by which climate affects demographic rates: blue is fertility, red is juvenile survival, orange is adult survival and purple is maturation rate. The dots stand for  $\beta_0 > 0$ , while square shows  $\beta_0 < 0$ . Panels show four life history strategies.

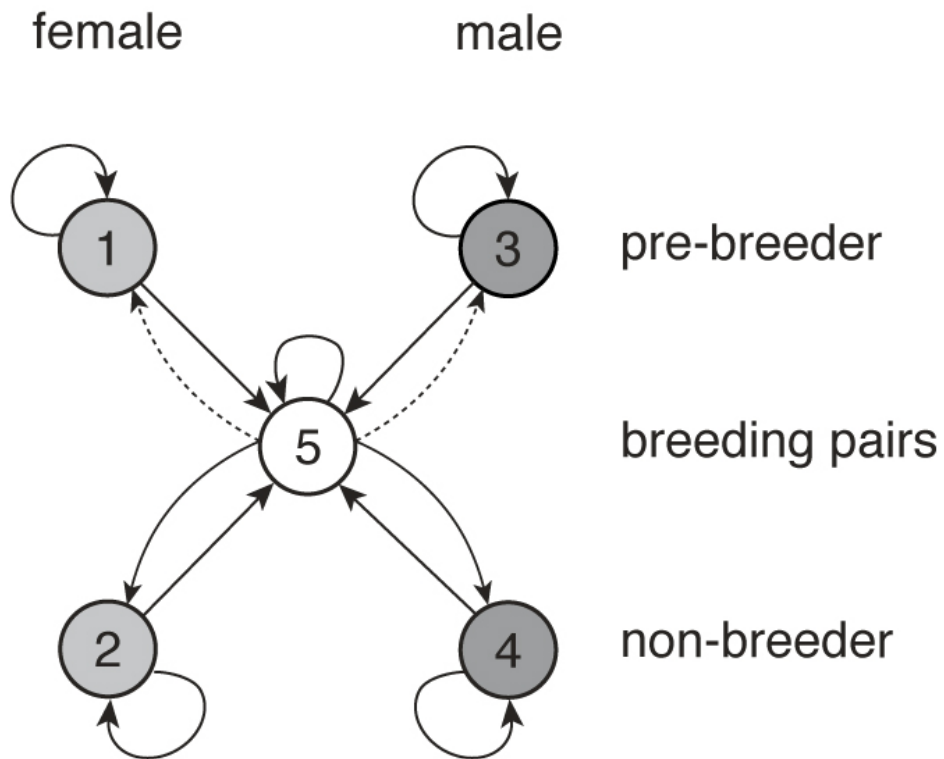


**Figure 7:** Annual life-cycle graph for the emperor penguin. It represents a two-sex model with males (black) and females (gray). Fertilities are shown by dotted lines, and the transitions between stages of individuals already present in the population are represented by solid lines (see Figure 1 from Jenouvrier *et al.* [2010] for more details on seasonal cycle of the emperor penguin).

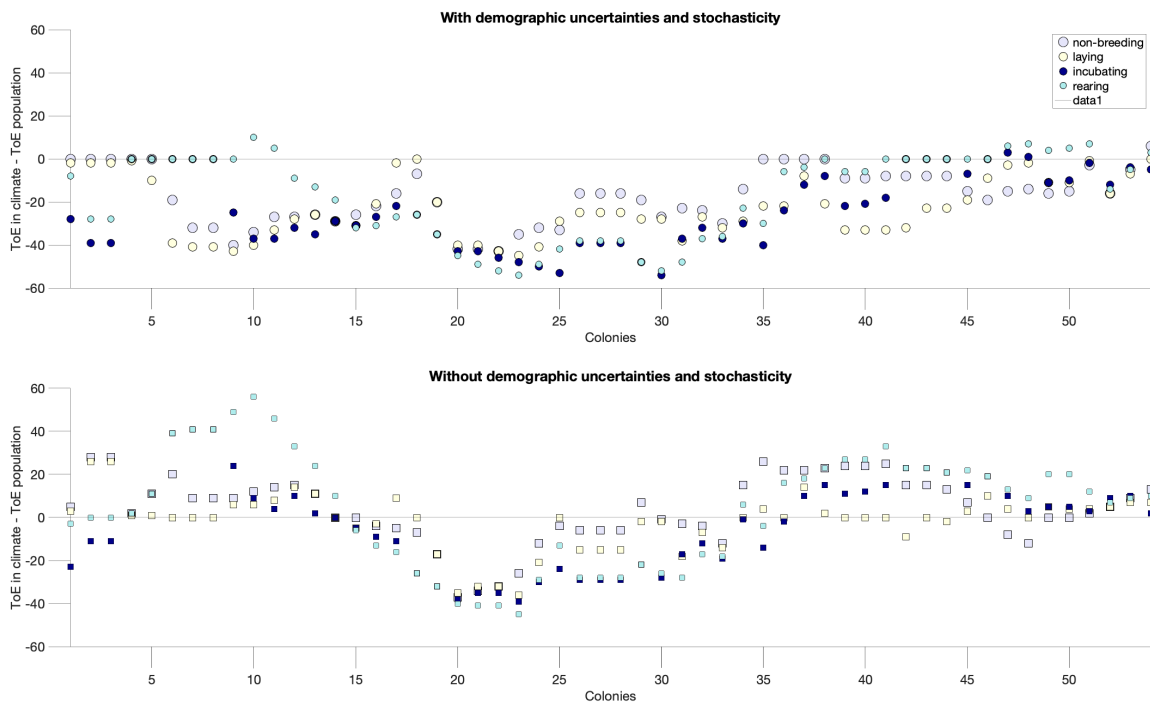


**Figure 8:** Difference between the time of emergence in sea ice and  $ToE_{pop}$  of emperor penguin ( $ToE_{climate} - ToE_{pop}$ ) for the 54 known colonies (x-axis) and four seasons (color). The calculation of  $ToE_{pop}$  accounts for  $var(\epsilon)$  generated by parameter uncertainty and process variance (i.e., environmental stochasticity) (a) or not (b).



**Table 1:** Glossary adapted from the IPCC definitions [Allen *et al.*, 2018]

---

<b>Climate change</b>
Change in the state of the climate that can be identified (e.g., by using statistical tests) by changes in the mean and/or the variability of its properties and that persists for an extended period, typically decades or longer. Climate change may be due to natural internal processes or external forcings such as modulations of the solar cycles, volcanic eruptions and persistent anthropogenic changes in the composition of the atmosphere or in land use.
<b>Climate model</b>
A numerical representation of the climate system based on the physical, chemical and biological properties of its components, their interactions and feedback processes, and accounting for some of its known properties. Climate models have structural differences for example, in their spatial resolution, complexity of parameterizations, and processes that are explicitly represented.
<b>Climate signal</b>
Variations in the state of the climate system that have an identifiable and statistically discernible structure in time and/or space, such as a long-term warming trend.
<b>Climate simulation</b>
A model simulation of the climate state. This can include the simulated response of the climate system to characterize historical climate conditions, climate predictions, or climate projections.
<b>Climate projection</b>
A simulated response of the climate system to a forcing scenario of future emission or concentration of greenhouse gases (GHGs) and aerosols, generally derived using climate models.
<b>Climate variability</b>
Variations in the mean state and other statistics (such as standard deviations, the occurrence of extremes, etc.) of the climate on all spatial and temporal scales beyond that of individual weather events. Variability may be due to natural internal processes within the climate system (internal variability), or to variations in natural or anthropogenic external forcing (external variability).
<b>Natural climate variability</b>
Climate fluctuations from unforced variability generated internally within the climate system (e.g. weather) or associated with external forces to the climate system (e.g. volcanoes).
<b>(Model) Ensemble</b>
A group of parallel model climate simulations. Ensembles made with the same model but different initial conditions characterize the simulation uncertainty associated with internal climate variability, whereas multimodel ensembles including simulations by several models also include the impact of model differences.
<b>Time of Emergence</b>
The time at which the signal of climate change emerges from the noise of natural climate variability.
<b>Emergence threshold</b>
A threshold at which climate change is considered to emerge.

---

**Table 2:** Demographic rates and outcomes for the four life history strategies (species in columns). Note that the fertility ( $F$  number of offspring that are produced per adult female in year  $t$ ) is reported here. The fecundity ( $b$  the number of offspring born per unit time per female) is discounted by the probability that an adult will actually survive from the time of the census to the birth pulse ( $F = bS_a$ ). The deterministic population growth rate is one for all species. The generation time (in years) is the mean age of parents (eq 14 of Bienvenu & Legendre [2015]), from the fundamental matrix the following demographic outputs are calculated: the mean life expectancy at birth and the mean remaining life at adulthood (eq 20 of [Roth & Caswell, 2018]); the probability to return to the adult state (from eq 47 of [Roth & Caswell, 2018] using state A on Fig. 2). Ex stands for extreme.

	species 1	species 2	species 3	species 4
	Life history strategies			
Reproductive strategy	Semelparous	Iteroparous	Iteroparous	Iteroparous
Developmental strategy	Precocious	Precocious	Delayed	Ex-Delayed
Survival strategy	Short-lived	Short-lived	Long-lived	Ex-Long-lived
	Demographic rates			
Annual fertility rate	5.06	3.00	1.00	0.50
Juvenile survival prob.	0.20	0.30	0.40	0.60
Adult survival prob.	0.03	0.39	0.83	0.93
Maturation rate	0.95	0.60	0.30	0.11
	Life history outcomes			
Generation time	2.04	2.77	7.40	16.30
Life expectancy at birth	1.21	1.47	2.39	4.17
Remaining life at adulthood	1.03	1.63	6.02	14.29
Probability to return to adult state	0.03	0.39	0.83	0.93

**Table 3:** Time of emergence, trend and variability of population growth rate, with its sensitivity to climate across all simulations for four life history strategies (species in row) and four demographic pathways by which climate affects demography rates (columns). Median of the time of emergence of population is denoted  $ToE_{pop}$ . At the time of emergence in the population: the median of the trend is  $T_{ToEpop}$ , the median of the variability in the forced environment is  $var_{ToEpop}$  and their ratio is  $T_{ToEpop}/var_{ToEpop}$  at  $ToE_{pop}$ ; and the median of the sensitivity of the population growth rate to climate is  $\frac{\partial \lambda}{\partial C_{C=ToEpop}}$ . Historical variability is denoted  $var(\lambda_t)$ .

	LINEAR				BELL SHAPE			
	$F$	$S_j$	$S_a$	$\gamma$	$F$	$S_j$	$S_a$	$\gamma$
$ToE_{pop}$								
species 1	133	134	125	140	133	126	125	146
species 2	102	64	70	87	106	68	73	86
species 3	116	73	56	63	107	75	60	65
species 4	123	99	54	54	120	105	58	58
$T_{ToEpop}/var_{ToEpop}$								
species 1	0.04	0.04	0.04	0.04	0.06	0.04	0.02	0.06
species 2	0.05	0.11	0.09	0.07	0.06	0.11	0.09	0.07
species 3	0.03	0.08	0.15	0.11	0.01	0.08	0.14	0.12
species 4	0.03	0.05	0.16	0.16	0.03	0.03	0.15	0.16
$T_{ToEpop}$								
species 1	0.0010	0.0032	0.0002	0.0003	0.0041	0.0067	0.0001	0.0085
species 2	0.0010	0.0021	0.0010	0.0008	0.0027	0.0021	0.0011	0.0018
species 3	0.0008	0.0008	0.0008	0.0006	0.0007	0.0010	0.0007	0.0005
species 4	0.0002	0.0004	0.0004	0.0003	0.0005	0.0004	0.0003	0.0002
$var_{ToEpop}$								
species 1	0.024	0.088	0.003	0.005	0.092	0.216	0.005	0.149
species 2	0.019	0.019	0.011	0.013	0.047	0.021	0.014	0.027
species 3	0.024	0.010	0.005	0.005	0.054	0.013	0.005	0.005
species 4	0.006	0.008	0.002	0.002	0.023	0.020	0.002	0.002
$\frac{\partial \lambda}{\partial C_{C=ToEpop}}$								
species 1	0.010	0.019	0.003	0.004	0.0018	0.0060	0.0002	0.0005
species 2	0.012	0.024	0.011	0.009	0.0022	0.0048	0.0023	0.0021
species 3	0.014	0.009	0.010	0.007	0.0025	0.0019	0.0021	0.0013
species 4	0.001	0.003	0.005	0.004	0.0005	0.0009	0.0011	0.0008
$var(\lambda_t)$								
species 1	0.025	0.108	0.003	0.006	0.005	0.022	0.001	0.002
species 2	0.019	0.019	0.011	0.014	0.003	0.004	0.002	0.003
species 3	0.031	0.010	0.006	0.005	0.007	0.002	0.001	0.001
species 4	0.008	0.009	0.003	0.002	0.002	0.002	0.001	0.000



## Supporting Information S1: additional figures

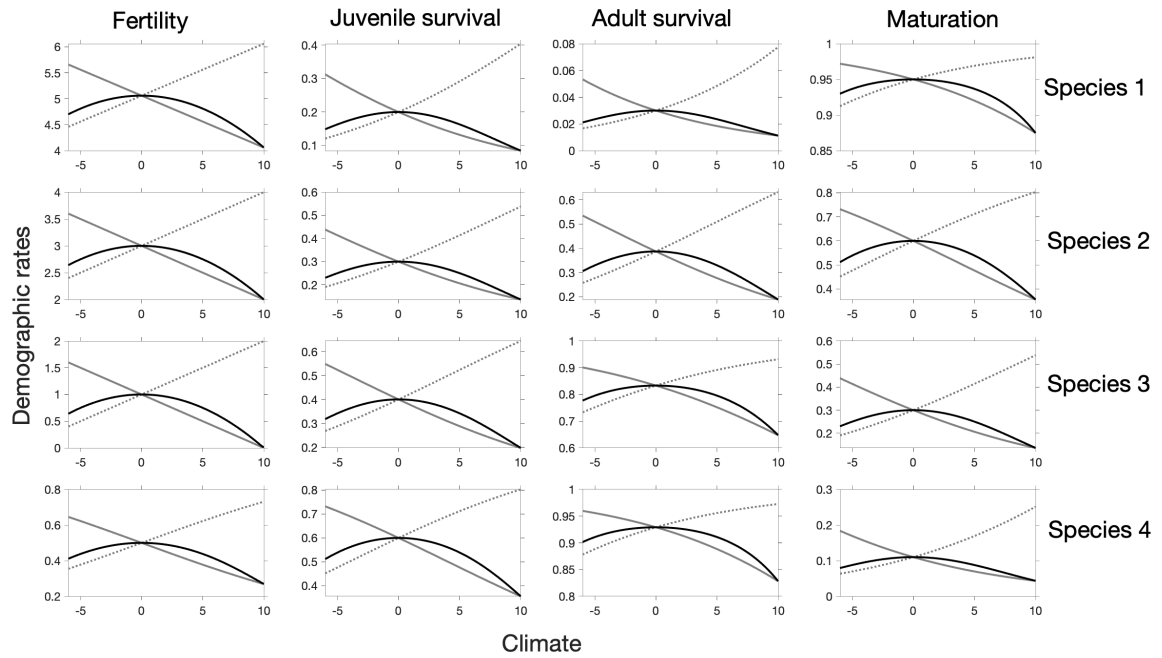


**Figure S 1:** Example of functional relationships that are linear or sigmoid with a slope  $\beta_0 = 0.1$ ,  $\beta_0 = -0.1$  for linear sigmoid functional relationship or  $\beta_0 = 0.01$  for bell shape relationships for each species (row panels) and each demographic rate (column panels).

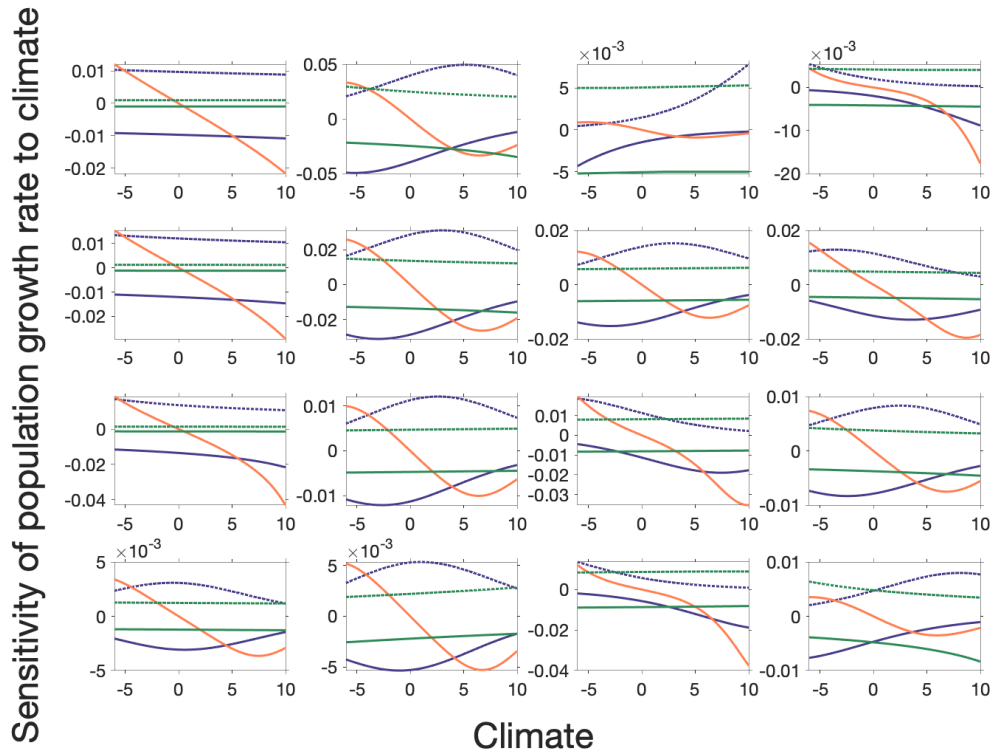


**Figure S 2:** Sensitivity of the population growth rate to climate for four life histories (panel in line: fast (species 1) to slow (species 4)) and demographic rates (panel in column: fertility, juvenile survival, adult survival and maturation rate) and different functional relationships between climate and demographic rates. Blue lines stands for linear on logit scale with  $\beta_0 = [-0.1/0.1]$ , orange line shows bell shape on logit scale with  $\beta_0 = -0.01$ , and green lines are linear on real scale  $\beta_0 = [-0.1/0.1]$ ,

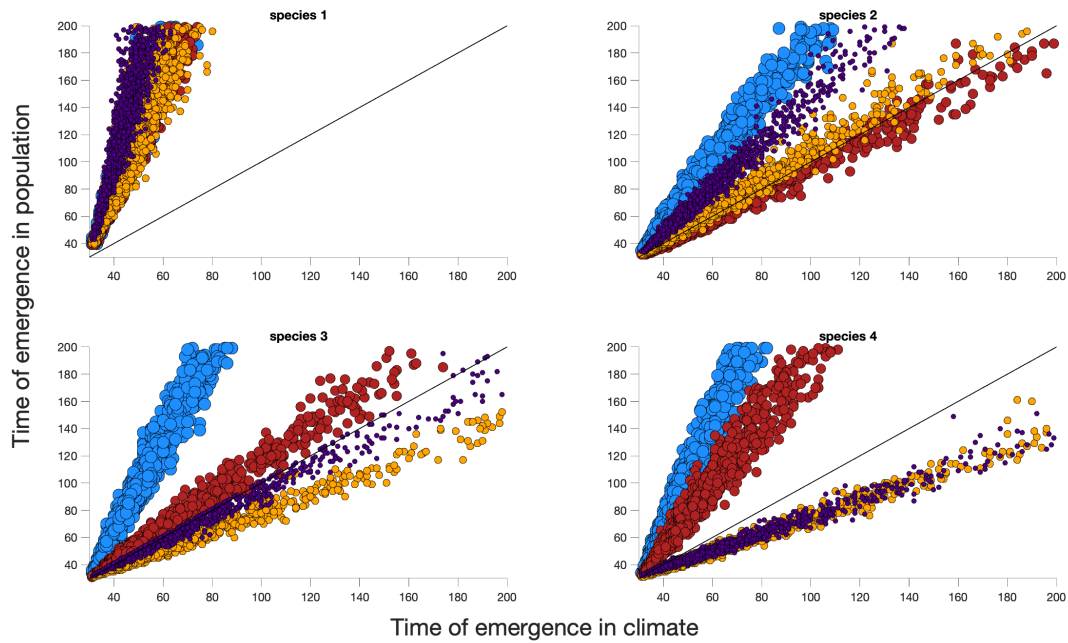


**Figure S 3:** Relationship between the time of emergence in climate (x-axis) and population (y-axis) for four life history strategies (panels), whereby climate affects only one demographic parameter at a time (colored dots: blue is fertility, red is juvenile survival, orange is adult survival and purple is maturation rate). The black line represent the time when the time of emergence in climate and population are equal. The functional relationships are linear or sigmoid. The emergence thresholds are defined by the 20th or 80th percentile values of the confidence interval. In that case, the system is likely highly sensitive to climate as severe impacts are thought to occur for lower percentile of the climate distribution experienced during the historical run.

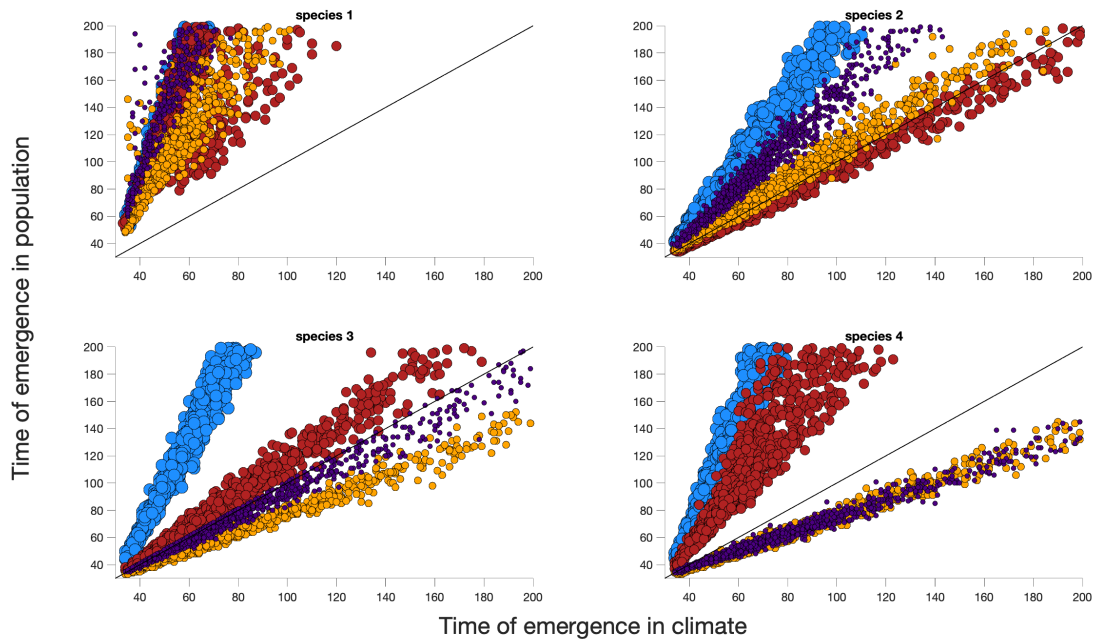


**Figure S 4:** Relationship between the time of emergence in climate (x-axis) and population (y-axis) for four life history strategies (panels), whereby climate affects only one demographic parameter at a time (colored dots: blue is fertility, red is juvenile survival, orange is adult survival and purple is maturation rate). The black line represent the time when the time of emergence in climate and population are equal. The functional relationships are linear on the real scale with  $\beta_0 = [-0.03 \ -0.02 \ -0.01 \ 0.01 \ 0.02 \ 0.03]$ .

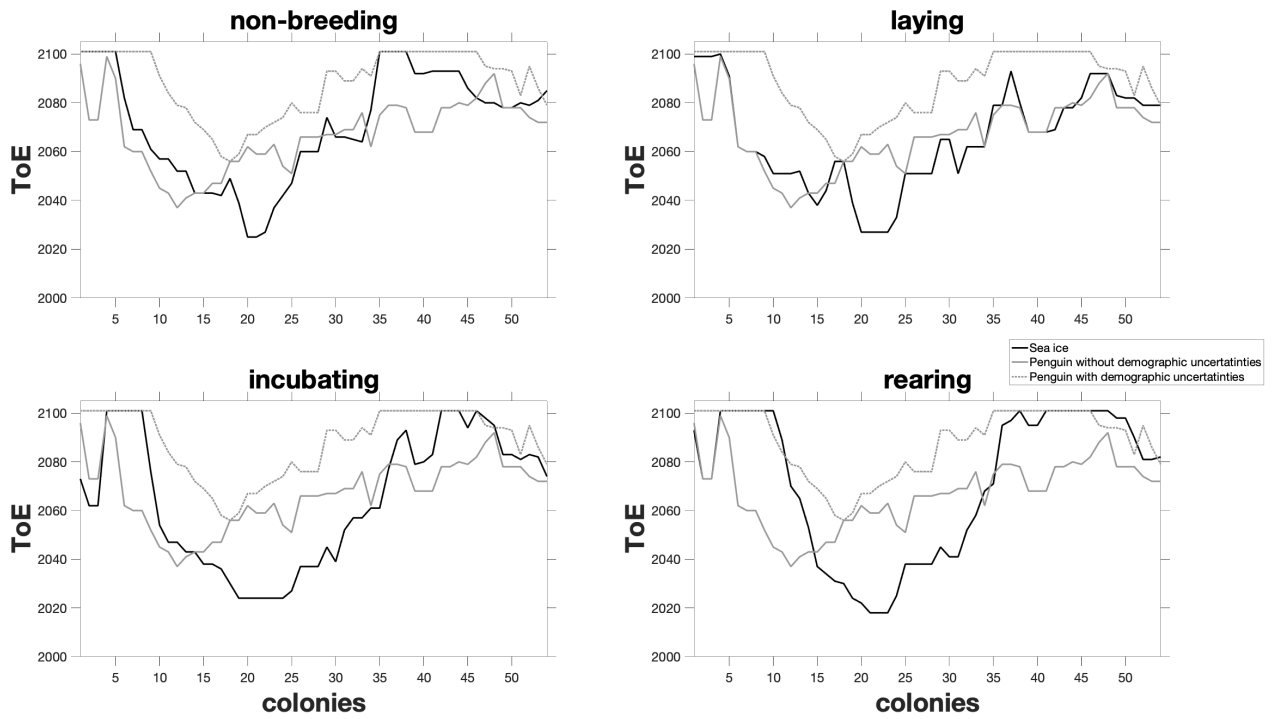


**Figure S 5:** Time of emergence in sea ice (black line) and in the population growth rate of emperor penguin (grey lines) for the 54 known colonies (x-axis) and season (panels). The calculation of ToE accounts for  $\text{var}(\epsilon)$  generated by parameter uncertainty and process variance (i.e., environmental stochasticity) (dotted line) or not (plain line).

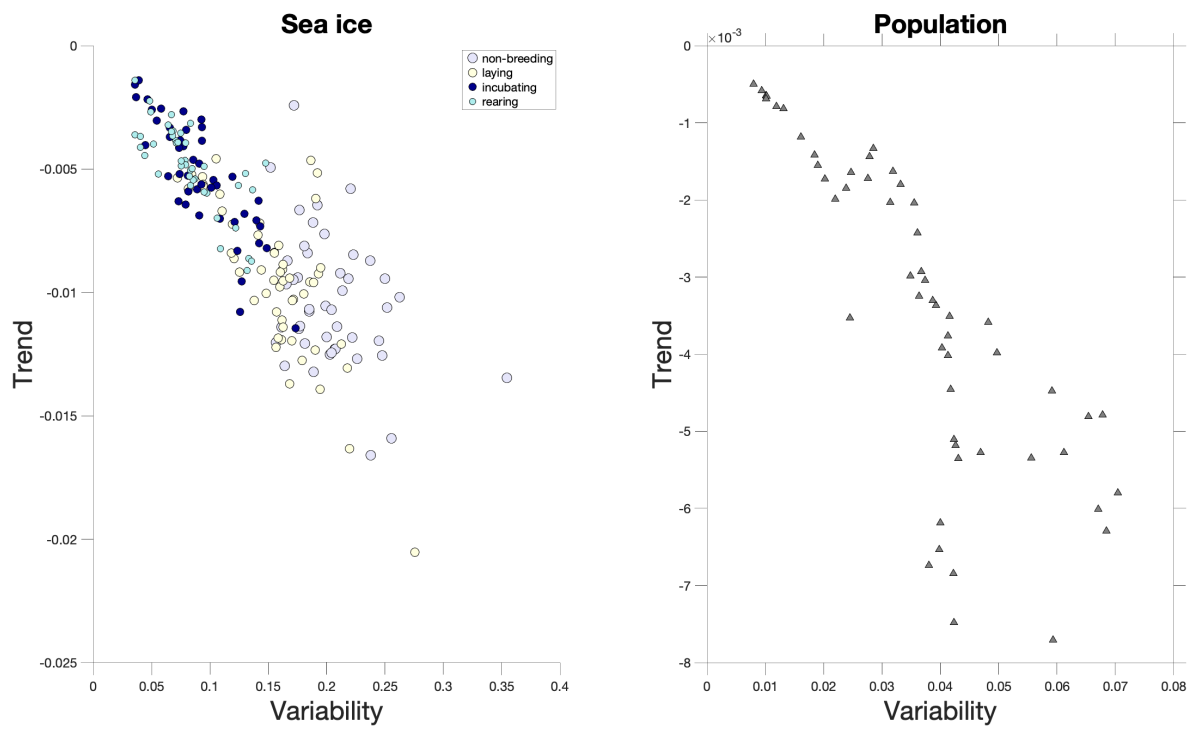


**Figure S 6:** Variability and trend at the time of emergence for sea ice (left panel) and for the population growth rate of emperor penguin (right panel) for the 54 known colonies (marker) and season (colors).

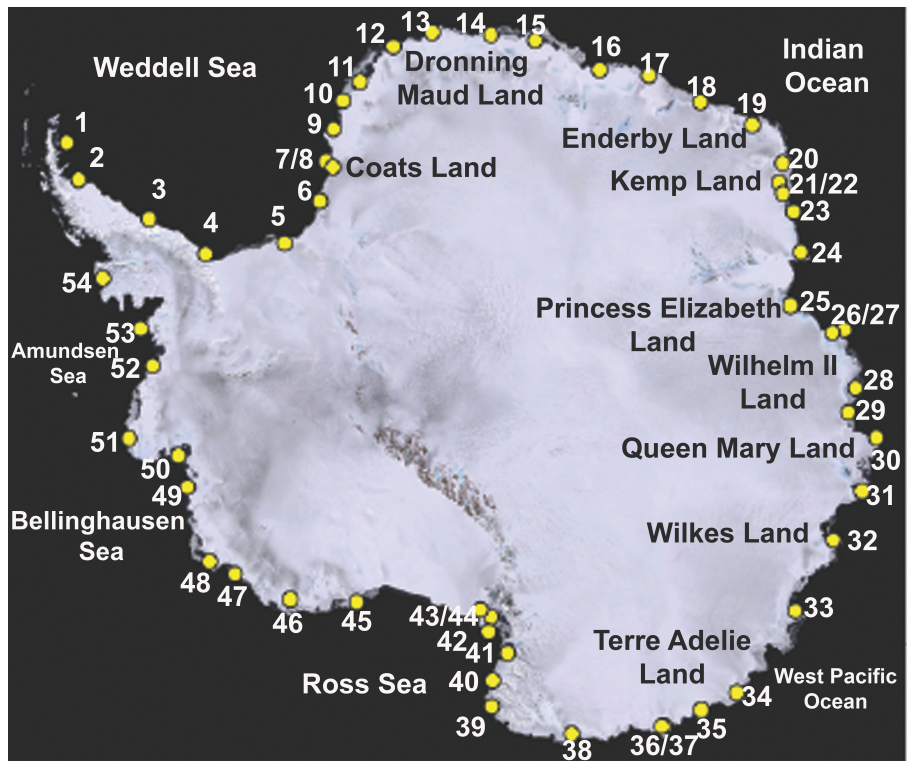


Figure S 7: Map of Emperor penguin colonies.

## Supporting Information S2: population variability in a stationary environment

Equation 13 shows that the variance in annual population growth rates  $\text{var}(\lambda_t)$  is linearly related to the climate variance  $\sigma^2$  in a stochastic stationary environment with small variations around a climate mean  $\bar{C}$ .

Figure S 8 shows the variance in annual population growth rates  $\text{var}(\lambda_t)$  as function of a mean climate  $\bar{C}$  for different life histories when climate affects the population through different demographic rates  $\theta_j$ . The functional relationships between climate and the demographic rate are linear on the real scale for fertilities (except species 4) or on the logit scale for other demographic rates. Let's assume that  $C$  represents temperature, and the population is stable for  $\bar{C} = 0$ .

The stationarity variability of the population growth rate varies as function of the mean climate in complex non-linear ways that depend on  $\frac{\partial \lambda}{\partial C}$  and the sign of the slope of the functional relationships between climate and demographic rates  $\beta_0$  that affects  $\frac{\partial \lambda}{\partial C}$ . The smallest  $\frac{\partial \lambda}{\partial C}$ , hence population growth rate variability, occurs for species 4 with an extreme long-lived history and the climate-dependent demographic rate of maturation rate regardless of the mean environmental conditions and functional relationships. Short-lived species (species 1 and 2) and the climate-dependent demographic rate of juvenile survival shows the largest  $\frac{\partial \lambda}{\partial C}$ , except for extreme positive mean climate. However, various patterns are observed between these extremes, which depend on the functional relationship between climate and demographic rates, the demographic rate by which climate affects population and the life histories of the species.

For example, for linear functional relationships between the fertility and climate (species 1-3), equation 13 becomes:

$$\text{var}(\lambda) = \beta_0^2 \sigma^2 \left( \frac{\partial \lambda}{\partial \theta_{i\theta_i=\bar{\theta}_i}} \right)^2 \left( \frac{\partial \theta_{i\theta_i=\bar{\theta}_i}}{\partial C_{C=\bar{C}}} \right)^2 = \beta_0^4 \sigma^2 \left( \frac{\partial \lambda}{\partial \theta_{i\theta_i=\bar{\theta}_i}} \right)^2 \quad (15)$$

If  $\beta_0 > 0$ ,  $\left( \frac{\partial \lambda}{\partial \theta_i} \right)^2$  increases as  $\bar{C}$  increases, and the variance in annual population growth

1217 rates is larger for warmer climate than colder climate. If  $\beta_0 < 0$ ,  $\left(\frac{\partial\lambda}{\partial\theta_i}\right)^2$  decreases as  $\bar{C}$   
1218 increases, and the variance in annual population growth rates is larger for colder climate  
1219 than warmer climate.

1220 For non-linear sigmoid functions, it is more complex, and depends on the specific  
1221 shape of the  $\left(\frac{\partial\lambda}{\partial\theta_i}\right)^2$  and the sign of  $\beta_0$ , specifically at which environment  $\bar{C}$  the maximum  
1222  $\left(\frac{\partial\lambda}{\partial\theta_i}\right)^2$  occurs. For example, for adult survival, the population growth rate variability  
1223 is larger for warmer climate than for colder climate for long lived species when  $\beta_0 < 0$   
1224 (species 3 and 4). However, the opposite pattern occurs for short lived species (species  
1225 1 and 2): the population growth rate variability is smaller for warmer climate than for  
1226 colder climate (Fig. S 8). These patterns are opposite when  $\beta_0 > 0$ .

1227 For bell shape functional relationships, the variance of the population growth rate is  
1228 smaller for comparable range of demographic rates (Table 2). Indeed, to obtain a realistic  
1229 range of demographic rates when  $\theta_{it} = g(y^* = \beta_0^*C_t^2 + \beta_1 + \epsilon_t)$  than when  $\theta_{it} = g(y =$   
1230  $\beta_0C_t^2 + \beta_1 + \epsilon_t)$  (Fig. S 1), the slope of the function  $y^*$  must be smaller:  $\beta_0^* < \beta_0$ . Hence  
1231  $\text{var}(\lambda)$  is smaller despite similar magnitude for  $\left(\frac{\partial\lambda}{\partial\theta_i}\right)^2$  for both function  $y$  and  $y^*$  (Fig. S  
1232 2).

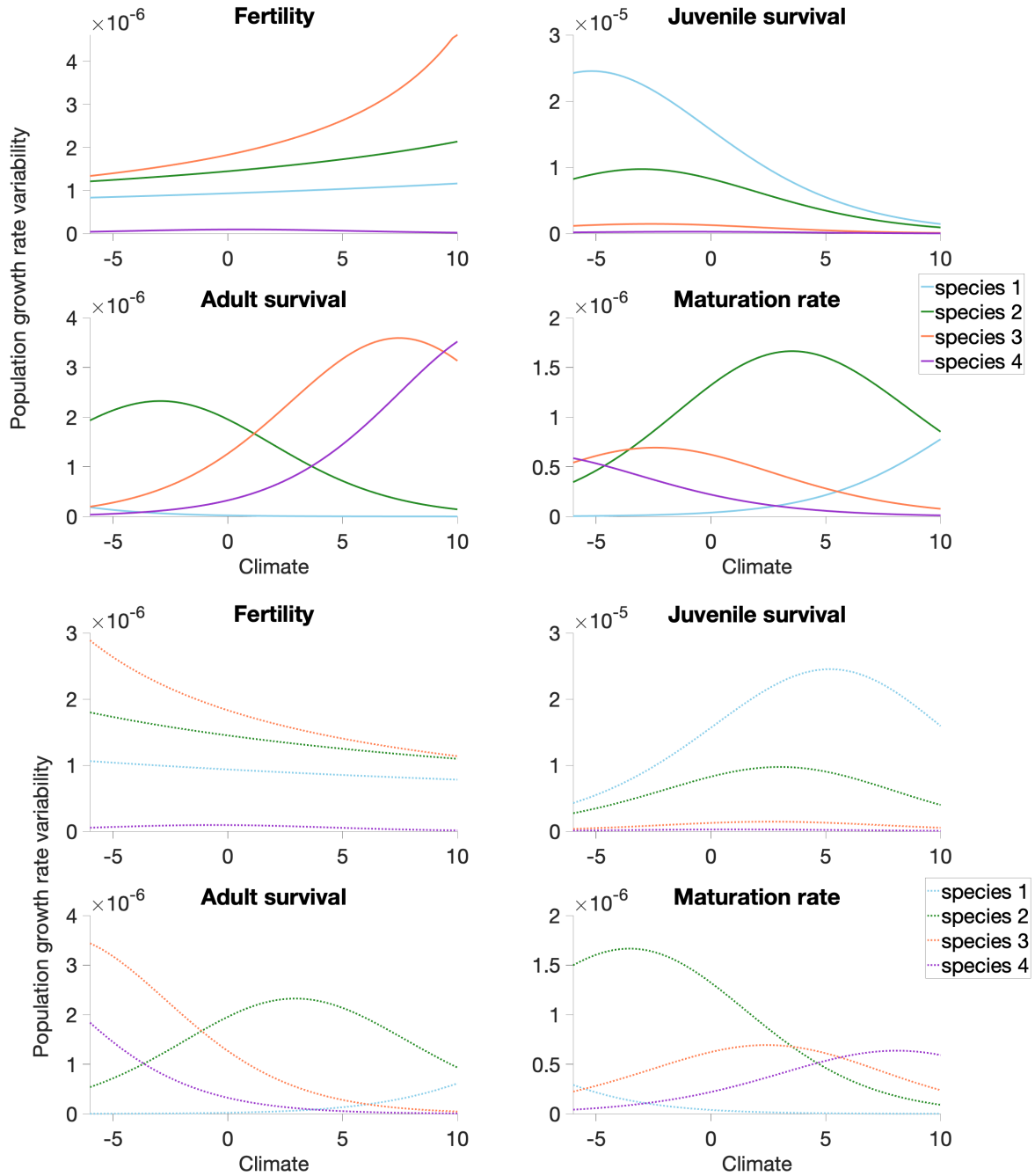


**Figure S 8:** Variability in annual population growth rates calculated from equation 8 across life histories. Panels show the variance in annual population growth rates  $\text{var}(\lambda_t)$  as function of the climate mean  $\bar{C}$  when climate affects population through different demographic rates: fertility, survival or maturation. Line color indicates different species along a gradient of fast-slow life histories, from fast (species 1) to slow (species 4). (a)  $\beta_0 = -0.1$  and (b)  $\beta_0 = 0.1$ .  $\sigma = 0.2$ .

1233 **Supporting Information S3: the sea ice-dependent-metapopulation model for em-**  
1234 **peror penguins**

1235

1236 Portions of the Supplementary Material are modified from Jenouvrier et al. (2010),  
1237 Jenouvrier et al. (2012), Jenouvrier et al. (2017) and Jenouvrier et al. (2021) under the  
1238 terms of the Publication Agreement with the University of Chicago Press, John Wiley &  
1239 Sons publications and Elsevier.

1240 Our sea ice-dependent-metapopulation model projects the population vector  $\mathbf{n}$ —comprising  
1241 the population size  $n_i$  in each colony  $i$ —from time  $t$  to  $t + 1$  using:

$$\mathbf{n}(t + 1) = \mathbf{D}[\mathbf{x}(t), \mathbf{n}(t)] \mathbf{F}[\mathbf{x}(t), \mathbf{n}(t)] \mathbf{n}(t) \quad (16)$$

1242 to indicate that the projection interval is divided into two main phases of possibly dif-  
1243 ferent duration: the reproduction phase ( $\mathbf{F}$ ) followed by the dispersal phase ( $\mathbf{D}$ )<sup>1</sup>. The  
1244 reproduction matrix  $\mathbf{F}$  is constructed using the Ricker model, which includes the intrinsic  
1245 population growth rate  $r_i(t)$ , which vary in time, and the carrying capacity of the colony,  
1246  $K_i$ , which is set to be constant over the entire time period. The dispersal phase ( $\mathbf{D}$ ) com-  
1247 bines various dispersal behaviors and dispersal events. The projection matrices  $\mathbf{D}$  and  
1248  $\mathbf{F}$  depend on both the current population density  $\mathbf{n}(t)$  and the habitat characteristics (in-  
1249 cluding sea ice concentrations anomalies),  $\mathbf{x}(t)$ , that vary among colonies and over time,  
1250  $t$ . The global population size at time  $t$  is given by  $N_t = \sum_i n_i(t)$ .

1251 **8.1 Reproduction phase**

1252 The reproduction matrix,  $\mathbf{F}$ , is constructed using the Ricker model including the in-  
1253 trinsic growth rate of each colony  $r_i(t)$  and the carrying capacity of each colony  $K_i$ . Neg-  
1254 ative density-dependence effects occur within crowded favorable habitats ( $r_i > 0$  and  
1255  $n_i > K_i$ ) while populations tend to go extinct within poor habitat colonies ( $r_i \leq 0$ ). Our

---

<sup>1</sup>Note on notation: In this paper, matrices are denoted by upper case bold symbols (e.g.  $\mathbf{F}$ ) and vectors by lower case bold symbols ( $\mathbf{n}$ );  $f_{ij}$  is the  $(i, j)$  entry of the matrix  $\mathbf{F}$ ,  $n_i$  is the  $i$ th entry of the vector  $\mathbf{n}$ .

1256 understanding of density dependence processes is extremely limited for emperor pen-  
1257 guins (see discussion in Appendix S1 of Jenouvrier *et al.* [2012]). Density dependence  
1258 may occur at breeding ground due to competition for space. For example, the Beaufort  
1259 Island colony growth is limited by the limited space available on the fast ice plate next to  
1260 the island [Kooyman *et al.*, 2007]. Competition for resources may also occur, although em-  
1261 peror penguins are able to forage over long distances over wide areas, probably reducing  
1262 intra-specific competition impact.

1263 **The intrinsic growth rate** For each projection interval  $t$ , the intrinsic growth rate of each  
1264 colony  $r_i(t)$  is projected by a nonlinear, stochastic, sea-ice dependent, two-sex, stage-  
1265 classified matrix  $\mathbf{A}[\theta[\mathbf{x}(t), \mathbf{n}(t)]]$ , including the demographic rates (reproduction and sur-  
1266 vival)  $\theta[\mathbf{x}(t), \mathbf{n}(t)]$  (described in more detail in Jenouvrier *et al.* [2010, 2012]). The life cycle  
1267 of this model is shown on Figure 7 and includes a sequence of seasonal behaviours (arrival  
1268 to the colony, mating, breeding) and accounts for differences in adult survival between  
1269 males and females as function of sea ice concentration anomalies  $\mathbf{x}(t)$ .  $\mathbf{A}[\theta[\mathbf{x}(t), \mathbf{n}(t)]]$  de-  
1270 pends on  $\mathbf{n}(t)$  because the reproduction is function of the proportion of males and females  
1271 within the population through mating processes [Jenouvrier *et al.*, 2010].

1272 **The carrying capacity** For emperor penguins, estimating the carrying capacity of the en-  
1273 vironment is a daunting task because population time-series are limited to a few colonies  
1274 around Antarctica, and no study thus far has reported the resources and breeding habi-  
1275 tat availability. Using the population projections from the stochastic sea-ice dependent  
1276 model that excludes density dependence [Jenouvrier *et al.*, 2017, 2014], Jenouvrier *et al.*  
1277 (2017) estimated the carrying capacity of each colony as  $K_i = 2N_0$ , with  $N_0$  the initial size  
1278 of the population observed in 2009 [Fretwell & Trathan, 2009; Jenouvrier *et al.*, 2014].

## 1279 **8.2 The dispersal phase.**

1280 Finally, the model includes inter-colony movements. A dispersal event includes the  
1281 three stages: (1) emigration from the resident colony, (2) search for new colony among  
1282 other colonies with an average dispersal distance  $d$  (transfer), and (3) settlement in a new

1283 colony. The duration of the transfer phase can vary, as the final settlement in a new colony  
 1284 may occur after several events (e.g., an individual may not settle in its first choice habitat  
 1285 if that habitat has reached its carrying capacity  $n_i \geq K_i$ ).

1286 In our model, movements of individuals among colonies are divided into two succes-  
 1287 sive dispersal events to account for a time-limited search. Indeed for emperor penguins  
 1288 the breeding season lasts 9 months, and thus the timing for prospecting other colonies  
 1289 during the non-breeding season is limited. During the first dispersal event ( $\mathbf{D}^1$ ) indi-  
 1290 viduals may select the habitat with highest quality (informed search) or settle in a ran-  
 1291 dom habitat. During the second dispersal event ( $\mathbf{D}^2$ ) individuals that reached a saturated  
 1292 colony leave and settle randomly in a new colony (see Fig. 1 in Jenouvrier *et al.* [2017]).  
 1293 The later is a way to account for a dispersal cost of gathering information for the informed  
 1294 search (see discussion in Jenouvrier *et al.* [2017]).

1295 The dispersal projection matrix  $\mathbf{D}$  is thus

$$\mathbf{D} := \mathbf{D}^2 \mathbf{D}^1. \quad (17)$$

1296 and each dispersal matrix  $\mathbf{D}^e$  is written

$$\mathbf{D}^e := \mathbf{S}^e[\mathbf{x}] \mathbf{M}^e[\mathbf{x}, \mathbf{n}_e] \quad (18)$$

1297 to indicate that matrices for searching behavior,  $\mathbf{S}^e$ , and emigration,  $\mathbf{M}^e$ , depend on the  
 1298 population size at the start of the event ( $n_e$ ) as well as the environmental conditions  $\mathbf{x}(t)$ .

1299 **The first dispersal event** The emigration rate for each colony  $i$  depends on the overall  
 1300 quality of the habitat, which is measured by the median of the realized population growth  
 1301  $\bar{r}_i^*$ . The emigration rate increases linearly from  $m^1 = 0$  at  $\bar{r} \geq 0$  to  $m^1 = 1$  at critical value

1302  $\overline{r_c^*} < 0$ . The emigration matrix thus only depends on the ratio  $\overline{\mathbf{r}^*(t)}/\overline{r_c^*}$ ,

$$\mathbf{M}^1 := \mathbf{M}^1 \left[ \frac{\overline{\mathbf{r}^*(t)}}{\overline{r_c^*}} \right]. \quad (19)$$

1303 A critical threshold  $\overline{r_c^*}$  close to 0, corresponds to high dispersion scenario while a larger  
 1304 negative threshold reflects low dispersion.

1305 Once individuals have left their colonies, we assume that they search for a new colony  
 1306 using two different behaviors: an informed searching behavior ( $\mathbf{S}_I$ ) and a random search-  
 1307 ing behavior ( $\mathbf{S}_R$ ).

1308 *The random search* assumes that dispersers randomly seek a colony within the limits  
 1309 of the maximum dispersal distance. Thus the probability of selecting a colony depends  
 1310 on the mean dispersal distance of the emperor penguin,  $d$ , and the matrix of distance  
 1311 between colonies ( $\text{dist}(i, j)$ ) included in the vector of habitat descriptors  $\mathbf{x}$ .

$$\mathbf{S}_R := \mathbf{S}_R[\mathbf{x}, d]. \quad (20)$$

1312 The matrix  $\text{dist}(i, j)$  corresponds to the coastal distance between colonies  $i$  and  $j$  derived  
 1313 from the location of know emperor penguin colonies.

1314 Conversely, *the informed search* assumes that dispersers search for the most favorable  
 1315 habitat they can reach; we use  $\overline{\mathbf{r}^*}$  as a descriptor of the quality of the habitat. Thus the  
 1316 informed search matrix is also a function of  $\overline{\mathbf{r}^*}$ :

$$\mathbf{S}_I := \mathbf{S}_I[\overline{\mathbf{r}^*(t)}, \mathbf{X}, d]. \quad (21)$$

1317 If the selected colony is not at carrying capacity, individuals settle in this new habitat.  
 1318 However, individuals are not able to settle in colonies that have reached their carrying  
 1319 capacities after the first dispersal event, and will conduct a novel search during the second  
 1320 dispersal event.

1321 **During the second dispersal event**, the surplus individuals leave and randomly settle in  
1322 another colony regardless of their dispersal strategy in their first event. Thus the emigra-  
1323 tion matrices depend on the carrying capacity  $\mathbf{K}$ , the population vector  $\mathbf{n}$  at the end of the  
1324 first dispersal event, and a random search matrix:

$$\mathbf{M}^2 := \mathbf{M}^2[\mathbf{K}, \mathbf{n}] \text{ and } \mathbf{S}^2 := \mathbf{S}_R. \quad (22)$$

1325 Note that because of our random settlement assumption during this second dispersal  
1326 event, individuals may come back to their resident colony if they first reached an over-  
1327 crowded colony.